



# Aerosol-associated non-polar organic compounds (NPOCs) at Jammu, India, in the North-Western Himalayan Region: seasonal variations in sources and processes

Shweta Yadav<sup>1</sup> · Sarita Bamotra<sup>1,2</sup> · Ankit Tandon<sup>2</sup>

Received: 24 October 2019 / Accepted: 9 March 2020 / Published online: 23 March 2020  
© Springer-Verlag GmbH Germany, part of Springer Nature 2020

## Abstract

Fine particulate (PM<sub>2.5</sub>) bound non-polar organic compounds (NPOCs) and associated diagnostic parameters were studied at Jammu, an urban location in the foothills of North-Western Himalayan Region. PM<sub>2.5</sub> was collected daily (24 h, once a week) over a year to assess monthly and seasonal variations in NPOC concentration and their source(s) activity. Samples were analyzed on thermal desorption-gas chromatography mass spectrometry to identify and quantify source-specific organic markers. Homologous series of n-alkanes, polycyclic aromatic hydrocarbons (PAHs), isoprenoid hydrocarbons and nicotine were investigated to understand the sources of aerosols in the region. The annual mean concentration of PM<sub>2.5</sub> during the sampling period was found higher than the permissible limit of India's National Ambient Air Quality Standards (NAAQS) and World Health Organisation (WHO) guidelines. The rise of concentration for PM<sub>2.5</sub> and associated NPOCs in summer season was attributed to enhanced emission. The n-alkane-based diagnostic parameters indicated mixed contributions of NPOCs from anthropogenic sources like fossil fuel-related combustion with significant inputs from biogenic emission. Moreover, high influence of petrogenic contribution was observed in summer (monsoon) months. The quantifiable amounts of isoprenoid hydrocarbons further confirmed this observation. Total PAH concentration also followed an increasing trend from March to June, and June onwards a sharp decrease was observed. The higher concentration of environmental tobacco smoke marker nicotine in winter months was plausibly due to lower air temperature and conditions unfavourable to photo-degradation. A clear dominance of low molecular weight PAHs was noticed with rare presence of toxic PAHs in the ambient atmosphere of Jammu. PAH-based diagnostic parameters suggested substantial contribution from low temperature pyrolysis processes like biomass/crop-residue burning, wood and coal fire in the region. Specific wood burning markers further confirmed this observation.

**Keywords** Ambient aerosols · Non-polar organic compounds · TD-GCMS · North-Western Himalayan Region

## Acronyms

ACL Average chain length

Responsible editor: Constantini Samara

**Electronic supplementary material** The online version of this article (<https://doi.org/10.1007/s11356-020-08374-3>) contains supplementary material, which is available to authorized users.

✉ Shweta Yadav  
shweta.evs@ujammu.ac.in

<sup>1</sup> Department of Environmental Sciences, Central University of Jammu, Bagla (Rahya Suchani), Samba, Jammu (J&K) 181143, India

<sup>2</sup> School of Earth and Environmental Sciences, Central University of Himachal Pradesh, Dharamshala, Kangra (H.P.) 176215, India

BBs	Box blanks
CA	Carbonaceous aerosols
CCN	Cloud condensation nuclei
C <sub>max</sub>	Carbon number of the most abundant n-alkane
CPCB	Central pollution control board
CPI	Carbon preference index
DCF	Dilution correction factor
Dp	Dew point
EBs	Equipment blanks
ETS	Environmental tobacco smoke
HMW	High molecular weight
IBs	Instrument blanks
KMO	Kaiser-Meyer-Olkin
LMW	Low molecular weight
MDRs	Molecular diagnostic ratios

MFC	Mass flow controller
NAAQS	National ambient air quality standards
NIST	National institute of standards and testing
NOAA-HYSPLIT	National oceanic and atmospheric administration-the hybrid single particle lagrangian integrated trajectory model
NPOCs	Non-polar organic compounds
NWHR	North-Western Himalayan Region
OCs	Organic compounds
PAHs	Polycyclic aromatic hydrocarbons
PBL	Planetary boundary layer
PCA	Principal component analysis
PM	Particulate matter
PNA	Petrogenic n-alkanes
RH	Relative humidity
RT	Retention time
SMVDS	Shri Mata Vaishno Devi Shrine
TD-GC-MS	Thermal desorption gas chromatography mass spectrometry
TNA	Total n-alkanes
TPAH	Total polycyclic aromatic hydrocarbons
WD	Wind direction
WHO	World health organization
WINS	Well impactor ninety-six
WNA	Wax n-alkanes
WS	Wind speed

## Introduction

Carbonaceous aerosol (CA) constituting ~30–70% mass of PM<sub>2.5</sub> present in the ambient atmosphere has crucial implications on regional and global climate as well as on human health (Jacobson et al. 2000; Pöschl 2005). The physical and chemical characteristics of CA reveal important information about their emission source(s) and transformation process(es) (Rodríguez et al. 2002; Patel and Rastogi 2018). Constituents of CA emitted from a variety of sources like combustion of fossil fuel, forest fires, vegetation burning, industrial effluents, exhaust from automobiles and aircraft emissions constitute a major fraction of aerosol mass in the environment (Novakov et al. 2000; Chen et al. 2016a; b). Factors contributing to the characteristics of carbonaceous aerosols include (1) nature and strength of emitting source(s), (2) incident solar radiations, (3) regional vegetation cover, (4) geomorphology of the region and (5) meteorological parameters (Yadav et al. 2013b, 2014; Zhang et al. 2018a). The studies involving investigation of CA have gained scientific interest recently due to its crucial role in inadvertent climate change and threats to human health. CA

alter the climate directly by absorbing and scattering solar radiation and indirectly by acting as cloud condensation nuclei and both of these phenomenon bears local, regional and global significance (Pöschl 2005; Ramachandran et al. 2006). The elemental (black carbon) component of CA has graphite like structure and strongly absorbs visible light resulting in positive radiative forcing thereby warming the atmosphere and impacting the climate (Andreae et al. 2006; Bond et al. 2013). However, large uncertainties exist in the case of organic fraction, which accounts for about ~25–75% of CA, due to the presence of various types of polar oxygenated compounds having ability to alter the cloud condensation nuclei (CCN) activity of CA (Petters and Petters 2016). The presence of thousands of potentially harmful compounds, many of which are known as carcinogenic (e.g. PAHs), in the organic fraction of CA pose a serious threat for human health (Rogge et al. 1993; 1994; Chen et al. 2016a; b).

The organic fraction that contains molecular tracers used in source apportionment studies consists of n-alkanes, n-fatty acids, n-fatty alcohols, n-alkanals, n-alkan-2-ones, long chain wax esters, dicarboxylic acids, polycyclic aromatic hydrocarbons (PAHs), diterpenoids, nicotine, anhydrosugars etc. (Chowdhury et al. 2007; Alves et al. 2019). These compounds can be used as tracers for identifying the source(s) of CA emission such as from biota, biomass/crop-residue burning, fossil fuel combustion and soil/road-side dust re-suspension (Van Drooge et al. 2018; Zhang et al. 2018a). The n-alkanes are relatively stable, non-polar and occur at high concentrations in urban regions due to their release from anthropogenic as well as biogenic processes (Young and Wang 2002; Yadav et al. 2013a). On the other hand, PAHs are produced as a result of incomplete combustion processes of organic matter and fossil fuels and are considered as environmental contaminants (Schauer et al. 2003).

Himalaya chain plays a unique and vital role in governing the climate of South East Asian region (Carrico et al. 2003). Increasing aerosol load over North-Western Himalayan Region (NWHR) has raised serious concerns (Kaushal et al. 2018; Kumar and Attri 2016; Huma et al. 2016; Pande et al. 2018; Yadav et al. 2019). Despite that, especially in India, the organic tracers have rarely been studied (Huma et al. 2016). Recently, Central Pollution Control Board (CPCB) of India has notified Jammu, an urban settlement in the foothills of NWHR as one of the non-attainment cities, where the particulate load exceeds permissible limits specified by National Ambient Air Quality Standards (NAAQS). Thus, there is a strong need of aerosol characterization particularly with regard to the accumulation mode ( $0.1 \mu\text{m} < d < 2.5 \mu\text{m}$ ) for the assessment of pollution, their source characterization and associated health risks (Kreidenweis et al. 2019).

In order to improve the existing knowledge about particulate air pollution in the NWHR, this study has been planned with the following objectives: (i) to investigate the chemical

characteristics of organic aerosols in the ambient environment, (ii) to quantify the aerosol-associated non-polar organic compounds (NPOCs), and (iii) to identify major source(s) of organic aerosols in the region on the basis of molecular tracers and diagnostic parameters/ratios. A systematic sampling campaign was conducted to collect twenty-four-hourly PM<sub>2.5</sub> aerosols on weekly basis at an urban location in Jammu, India. PM<sub>2.5</sub> samples were characterized for homologous series of n-alkanes, PAH, isoprenoid hydrocarbons, Environmental Tobacco Smoke (ETS) markers and other source specific organic tracers. Further, the correlations between meteorological parameters and the organic fraction of CA were explored to identify major processes and source contribution to organic aerosol load in the region.

## Materials and methods

### Sampling details

#### Description of sampling site

In this study, PM<sub>2.5</sub> sampling was done at Shastri Nagar (31° 14' 29" N, 77° 2' 12" E; 327 m amsl), an urban location in the Jammu city lying over irregular low-height ridges in the foothills (Shivaliks) of NWHR. Figure 1 shows the sampling location. The sampling site is situated near the National Highway (NH-1A) and is around 2.5 km away from the Jammu (IXJ) airport. Basically, it is a residential site but may have influences of vehicular traffic and other anthropogenic emissions. The sampler was placed on the rooftop of a building at around 10-m height from the ground and was not under any shade of tree or building.

#### Sample collection

PM<sub>2.5</sub> (aerodynamic diameter  $\leq 2.5 \mu\text{m}$ ) samples were collected on pre-baked and pre-weighed 47-mm quartz-microfiber filter matrix using a Well Impactor Ninty Six (WINS) based Fine Particulate Sampler equipped with a Mass Flow Controller (Envirotech, APM 550 MFC) that operates at a constant flow rate of 16.7 L/min, i.e. 1 cubic meter per hour. Twenty-four hourly PM<sub>2.5</sub> sampling was done once in a week (mid-week days) from October 2015 to February 2017. Automobile traffic flow and other anthropogenic activities are expected to be best represented on mid-week days, selected for the sample collection. Field blanks were collected by keeping the blank filters in the sampler, for the same duration and were exposed to the similar environmental conditions. Prior to their weighing, all PM<sub>2.5</sub> deposited filter papers were kept into desiccators filled with silica gel and after weighing were stored under controlled temperature and relative humidity conditions in clean petridishes, wrapped with aluminium

foil and refrigerated at  $-20 \text{ }^\circ\text{C}$  until analysis. Field blanks and PM<sub>2.5</sub> deposited filters were weighed before and after sampling on a well-calibrated electronic microbalance (Sartorius BSA 224S-CW).

### Analysis of aerosol samples using thermal desorption gas chromatography mass spectrometry

Analysis of organic tracers was done using well-established thermal desorption gas chromatography mass spectrometry (TD-GC-MS) method, which has been optimized and discussed elsewhere (Yadav et al. 2013a, b, 2014; Huma et al. 2016). The uniform aerosol filter discs (25-mm diameter) were further longitudinally cut into strips for easy insertion into the TD tubes (SS PE ATD Tube 25,049; Supelco, Bellefonte, PA, USA). The TD tubes were pre-baked before use and purged with high purity (99.990%) N<sub>2</sub> gas. The sample stripes (with silane treated glasswool plug at both ends) were loaded in the TD tubes for analysis.

Thermal desorption system TD-20 coupled with gas chromatograph mass spectrometer model GCMS-QP2010 Plus (Shimadzu, Japan) was used for analysis of organic tracers. Sample processing time/sample in TD unit was 15 min under pre-set operating conditions: 60 ml/min of gas flow; valve temperature of 250 °C; trap heat temperature of 280 °C; trap cool temperature  $-20 \text{ }^\circ\text{C}$  and interface heat temperature 250 °C. Table 1 shows the stepwise linear temperature ramping steps. High purity helium (99.999% purity) was used as a carrier gas at an auto-adjusted flow rate. The total run time for each sample in GCMS was 57 min.

### Quality assurance and quality control

The optimization of injection port temperature and thermal desorption procedure is important for determination of organic tracers (Schnellekreis et al. 2005). Several comparison studies in the past have shown good agreement between thermal desorption (TD) method and traditional method of solvent extraction; however, there are some limitations of TD method (Van Drooge et al. 2009; Wang et al. 2019 and references therein). Once the TD method is established, it is found to be advantageous in terms of lesser changes of contamination from solvents as well as lesser time consumption in sample preparation. The method used here has already been tested and optimized for optimal chromatographic resolution with reproducible mass spectra of targeted organic tracers (Yadav et al. 2013a, b, 2014; Huma et al. 2016). Samples were run in triplicate to ensure reproducibility. Analytical precision of  $\sim 5\%$  was ascertained and different sets of recovery experiments were performed to optimize the protocol for the detection and maximum desorption of organic compounds. In all, a recovery of 98% and more was achieved. Box blanks (BBs),

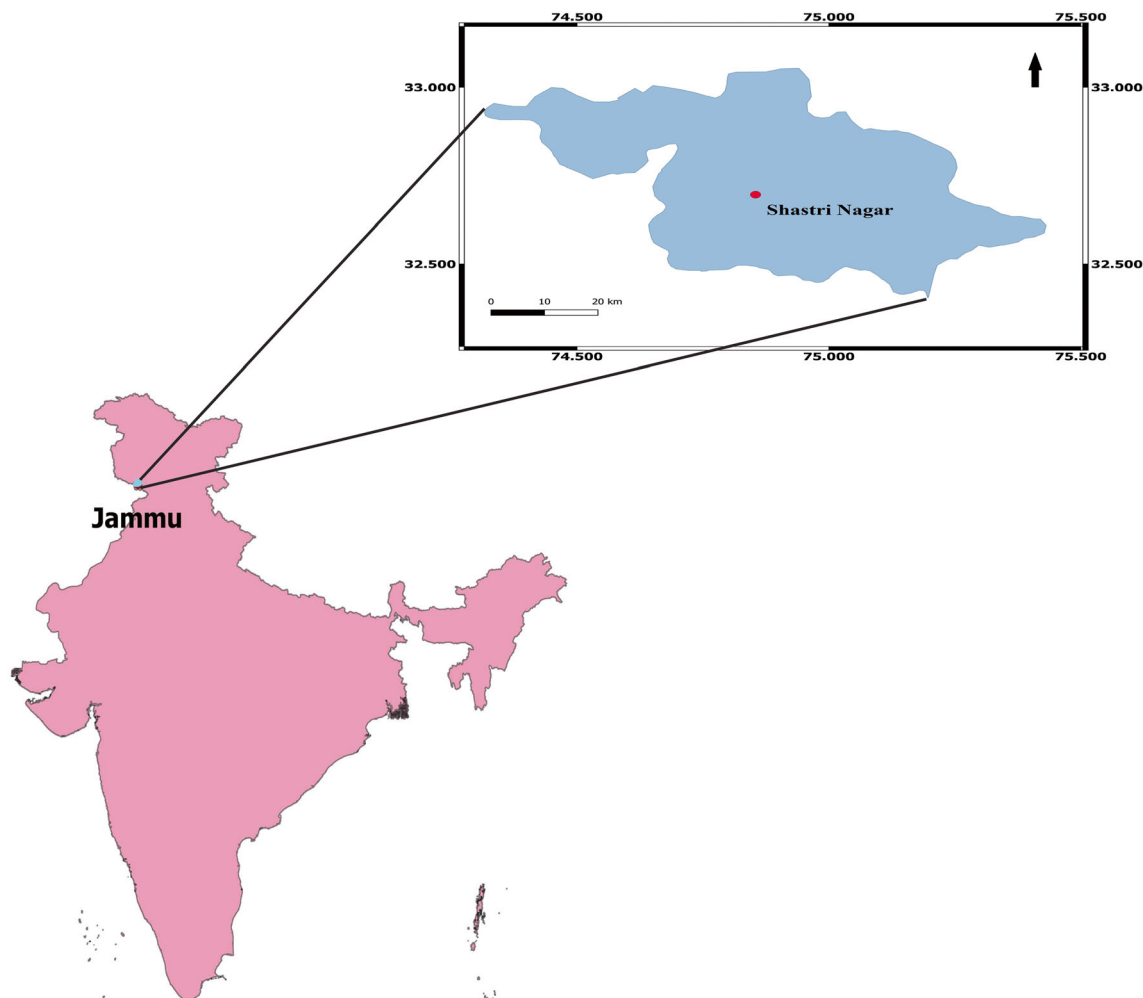


**Fig. 1** Map showing sampling location at Shastri nagar, Jammu, Jammu & Kashmir

instrument (TD-GCMS) blanks (IBs) and equipment blanks (EBs) aka field blanks were analyzed with same program in each batch run of aerosol samples to ensure quality assurance and quality control (QA/QC) during the analysis. BBs were picked from the filter box and were pre-baked and pre-weighed for analysis. IBs were analyzed by running the program with empty SS tubes. One IB was analyzed in the start of each day to check instrument contamination (if any) and then one IB was analyzed after every batch of 5 samples to check the sample to sample carryover. Another IB was run in continuation when the carryover was noticed in first IB and the

sample repeats were performed accordingly to ensure the best possible analysis. EBs (field blanks) were collected by keeping the pre-baked and pre-weighed blank filter paper in the air sampler (without switching the sampler on) for same sampling duration (24 h) as for collected samples. These EBs were then analyzed using baked and cleaned SS tubes.

### Analysis of organic species

Quantitative determination of non-polar organic compounds involved spotting of the molecular ion peak ( $M^+$ ) and comparison of retention times (RT) with reference standards. Further, the fragmentation pattern was matched with inbuilt National Institute of Standards and Testing (NIST) and Wiley mass spectral libraries. Compounds with similar molecular weights were confirmed on the basis of calibration standards (Silverstein et al. 2014). Polar organic markers like levoglucosan and dehydroabietic acid were also identified in some samples; however, no derivatization step was performed to quantify these markers.

**Table 1** Stepwise linear temperature ramping program used in TD-GCMS analysis

Steps	Rate	Initial temperature	Final temperature	Hold time
Step 1		80 °C	–	1 min
Step 2	5 °C min <sup>-1</sup>	80 °C	110 °C	3 min
Step 3	5 °C min <sup>-1</sup>	110 °C	320 °C	5 min

### Diagnostic parameters and isomeric ratios

Diagnostic parameters were used to assess the nature of contributing source types: Carbon Preference Index (CPI), carbon number of the most abundant n-alkanes ( $C_{max}$ ), the contribution of wax n-alkanes from plants (WNA%), petrogenic n-alkanes (PNA%) and higher plant n-alkane average chain length (ACL). CPI denotes the odd to even carbon number predominance and suggests the contributions arising from biogenic and petrogenic inputs (Bray and Evans 1961; Abas and Simoneit 1996; Alves et al. 2014); it is calculated by using the following relation:

$$CPI = \frac{\sum_{i=13}^{35} C_i}{\sum_{k=12}^{34} C_k}$$

where  $i$  = odd and  $k$  = even carbon number n-alkane concentration in above relation.

WNA is calculated by subtracting the average of next higher and previous lower even numbered carbon n-alkane congener present in the sample, negative values are taken as zero; the following expression was used for the calculations of WNA and its percentage:

$$WNA_{-C_n} = [C_n] - \left[ \frac{C_{n-1} + C_{n+1}}{2} \right]$$

where  $n$  stands for odd carbon number

$$WNA\% = \frac{\sum WNA_{-C_n}}{\sum NA} \times 100$$

WNA% gives the percentage contribution of wax n-alkanes in the sample, where  $\sum WNA_{-C_n}$  is the concentration sum of wax n-alkane contribution arising from all odd n-alkanes, and  $\sum NA$  is the concentration sum of total n-alkanes. Higher values of WNA% indicate contribution from biogenic sources whilst n-alkanes with odd carbon number (> 25) are emitted from the vegetation containing leaf composites (Sarti et al. 2017). Aerosol-associated n-alkanes can originate either from plant waxes or from petroleum source(s), percentage of petrogenic n-alkanes (PNA%) can be calculated as:

$$PNA\% = 100 - WNA\%$$

The most abundant n-alkane of the homologous series is  $C_{max}$ . The value of  $C_{max}$  serves as a marker to differentiate between various sources like diesel exhaust, higher plant waxes etc. (Yadav et al. 2013a).

ACL index, a proxy for temperature and humidity related emissions of n-alkanes from plants represent the average number of carbon atoms per molecule based on the abundance of higher odd carbon numbered plant n-alkanes (Huma et al. 2016), ACL is expressed as:

$$ACL(n\text{-alkanes}) = \frac{23X(C_{23}) + 25X(C_{25}) + \dots + 33X(C_{33}) + 35X(C_{35})}{(C_{23}) + (C_{25}) + \dots + (C_{33}) + (C_{35})}$$

Molecular diagnostic ratios (MDRs) used to understand the monthly and seasonal variations in the source(s) of NPOCs include ratio between Anthracene (ANT) and Phenanthrene (PHE)—[ANT/(ANT + PHE)] and ratio between Fluoranthene (FLT) and Pyrene (PYR)—[FLT/(FLT + PYR)]. Isoprenoid hydrocarbon-based ratio between Pristane and Phytane (Pr/Ph) was also used for source apportionment of fine particulates. However, the PAH-based ratios are reported to undergo photo-chemical degradation and inter-source variation in emission due to their high specific reactivity (Van Drooge et al. 2018).

### Organic molecular markers as source tracers

The quantified source specific organic compounds, to assess the biogenic, petrogenic and pyrogenic inputs to PM<sub>2.5</sub> load, were homologous series of n-alkanes (C11–C35), 2 ring PAHs [naphthalene (NAP)]; 3 ring PAHs [acenaphthylene (ACY), acenaphthene (ACE), fluorene (FLU), phenanthrene (PHE), anthracene (ANT)]; 4 ring PAHs [fluoranthene (FLT), pyrene (PYR), benzo(a)anthracene (BAA), chrysene (CHY)]; 5 ring PAHs [benzo(k)fluoranthene (BKF)]; 3 isoprenoid hydrocarbons [farnesane (Fr: 2,6,10-trimethyldodecane), pristane (Pr: 2,6,10,14-tetramethylpentadecane) and phytane (Ph: 2,6,10,14-tetramethylhexadecane)]. The multi-temporal variation in other organic tracers viz. isoquinoline, methylphenanthrene and certain wood burning markers [levoglucosan; retene; dehydroabietic acid] has been investigated. Nicotine a well-known tracer for environmental tobacco smoke (ETS) was also determined.

### Homologous series of n-alkanes

Homologous series of n-alkanes are known to retain the signatures of their sources and are considered as ubiquitous and the most abundant organic compounds present in the atmosphere acting as molecular markers (Alves et al. 2014; Javed et al. 2019). Aerosol-associated n-alkanes are relatively long-lived and chemically stable organic compounds. Being hydrophobic n-alkanes also have implications on the CCN activity of mixed composition particles present in different morphologies (Tandon et al. 2019). Total n-alkanes (TNA) are emitted from sources that can be categorized into biogenic (leaf epicuticular waxes, vegetation debris, soil dust, leaf abrasion, microorganisms etc.) and petrogenic sources (fossil fuel combustion, biomass/crop-residue burning, waste burning, tail pipe exhaust, tire wear and cooking operations etc.) (Alves et al. 2014).

## Polycyclic aromatic hydrocarbons

Polycyclic aromatic hydrocarbons (PAHs) exist as semi-volatile species in both gas as well as particulate phases. PAHs are emitted in the atmosphere primarily as by-products of incomplete combustion processes (Martins et al. 2016; Alves et al. 2017). PAHs are emitted from diverse sources: fossil fuel combustion, biomass burning, open straw and crop refuse burning, cigarette smoking, agricultural and municipal solid waste burning, waste incineration, environmental tobacco smoke, coke and metal production, oil refining, evaporative losses through oil spillage or refilling of tanks and natural sources like forest fires and volcanic eruption (Schauer et al. 2003; Chen et al. 2016a; b). These multi-ring compounds can be categorized as low molecular weight PAHs (LMW with 2–3 aromatic rings) which are volatile with more presence in the vapour phase than particle phase, and high molecular weight PAHs (HMW with 4 or more aromatic rings) which mostly occur in the particle phase (Sarti et al. 2017). The mutagenic and carcinogenic properties of PAHs pose major health concern (Yadav et al. 2013a; Li et al. 2019; Masih et al. 2019).

Most previous studies have focussed on HMW PAHs but recent studies have shown the toxic effects of LMW PAHs on lung function (Siegrist et al. 2019). LMW PAHs are abundant in second hand smoke and are also emitted by evaporative losses. Among high molecular weight PAHs, the 5-ring benzo[k]fluoranthene (BkF) serves as a marker for vehicular exhaust and 4-ring PAHs fluoranthene and pyrene for coal combustion. Phenanthrene, fluoranthene and pyrene can act as markers for emissions rising from combustion of conifers, angiosperms and grasses, respectively; also the combination of fluoranthene, fluorene and pyrene has been used as marker for oil combustion, with pyrene as an individual marker for emissions coming from diesel emissions (Khan et al. 2015).

Some individual PAHs, when correlated with other compounds, e.g. retene (present in the atmosphere in both gas and particulate phase) with high concentration of resin acids, pyrene, fluoranthene and phenanthrene serves as excellent signatures for combustion of coniferous softwood (Mikuška et al. 2015; Křůmal et al. 2017). Also certain combinations of PAHs like those of fluoranthene-pyrene with fluorene and phenanthrene are found to be prevailing in the emissions originating from burning of oil and incineration processes (Yadav et al. 2013a; Mikuška et al. 2015).

## Environmental tobacco smoke and other source-specific organic tracers

Environmental tobacco smoke (ETS), consisting of a diluted and aged mixture of side-stream smoke (smoke between puffs during tobacco products smoking), and originating from the mainstream smoke (exhalation of smoke from active smokers), is a well-known potential contributor to ambient pollution. Nicotine

(3-[(2S)-1-methylpyrrolidin-2-yl] pyridine), a constituent of ETS (Thompson et al. 1989) is a colourless, pale yellow, oily hygroscopic fluid found in the leaves of *Nicotiana tabacum*. It belongs to the group of nitrogen-containing alkaloid species and is found at high concentrations in ETS thus it is used as a tracer for ETS (Pankow 2001; Yadav et al. 2014). The chemical constituents of ETS, apart from nicotine, also include n-alkanes, branched (2-methyl-(iso-) and 3-methyl-(anteiso-) alkanes from C<sub>29</sub> to C<sub>33</sub>, PAHs, steranes and other nitrogen-containing compounds. Isoquinoline (C<sub>9</sub>H<sub>7</sub>N), is a toxic N-containing compound similar to nicotine is one of the constituents of environmental tobacco smoke (ETS) (Huma et al. 2016). However, these organic species have multiple sources and thus nicotine is used as the best source-specific tracer for ETS (Chalbot et al. 2012).

Other organic markers spotted in this study include isoquinoline, retene, levoglucosan, methylphenanthrene and dehydroabietic acid. Retene, an alkylated phenanthrene [(1-methyl-7-isopropyl phenanthrene), is produced during the incomplete combustion of resin containing coniferous softwood (Patel and Rastogi 2018) and serves as a molecular marker for wood combustion (Urban et al. 2016). Besides retene, other biomass burning tracers were detected during the course of this study; they were levoglucosan (monosaccharide anhydride) and dehydroabietic acid. Levoglucosan is a chemically stable species present in the atmosphere and emitted during the process of thermal splitting/alteration of cellulose, hemicellulose containing material at temperatures  $\geq 300$  °C. It is an established marker for biomass burning viz. combustion of wood for heating/cooking etc. (Vicente et al. 2011; Alves et al. 2014; Nirmalkar et al. 2015; Martins et al. 2016; Mancilla et al. 2016; van Drooge et al. 2018). Primarily emitted as clusters of gaseous molecules and associated to suspended particles, as temperature drops, levoglucosan becomes quite persistent (Nirmalkar et al. 2015). Dehydroabietic acid belongs to the group of resin acids, i.e. diterpenoid carboxylic acids emitted during the combustion process of coniferous woods (Alves et al. 2014). The group of three organic tracers viz. levoglucosan, dehydroabietic acid and retene act as unique markers for biomass (wood) burning, with the latter two having same source of emission, i.e. from coniferous woods and the former being present in both coniferous and deciduous woods. An earlier study (Rinehart et al. 2006) reported strong correlation between retene and dehydroabietic acid, indicating their common source of origin. Methylphenanthrenes (Me-Phe) is emitted during evaporation of fuels (Pant et al. 2015). These alkylated PAHs are emitted from more mature organic matter (petrogenic sources) and the various sources of Me-Phe can be categorized as (a) the roadway evaporation of fossil fuel drippings; (b) losses due to evaporation during refuelling of motor vehicles; and (c) unleashing of frying oils from restaurants. So, keeping in mind their prevalence in particulate matter and relation with unburned petroleum fuel,

these Me-PAHs, particularly monomethylated phenanthrenes (Me-Phe) have been stressed upon for their inclusion into the countries ambient air monitoring programme. The ratio of Me-Phe/Phe has been used for identifying sources of PAHs emitted from vehicular traffic (Kavouras et al. 1998).

### Meteorological variables

Meteorological variables such as depth of planetary boundary layer (PBL), surface air temperature (T), dew point temperature (Dp), relative humidity (RH), wind speed (WS) and wind direction (WD) were retrieved from Air Resource Laboratory, National Oceanic and Atmospheric Administration (<http://www.arl.noaa.gov/READYamet.php>). Combined weekly values of PBL (m), T (°C), RH (%) and WS (knots) were used to derive monthly average values. The values obtained from the data were averaged and plotted for each of these variables.

### Principal component analysis

Statistical analysis is commonly used in source apportionment studies (Yadav et al. 2016). In this study, Principal component analysis (PCA) was performed on the mass concentration data-set of NPOCs to identify their possible sources over the Jammu town in NWHR. The randomness in the data-set was ascertained by performing Kaiser-Meyer-Olkin (KMO) test. Starting with the correlation matrix for various NPOCs studied, Kaiser-Varimax rotation was applied on the initial solution so that the sum of the variance of the squared loadings, where ‘loadings’ means correlations between variables and principal components gets maximized. This usually results in component loadings close to one for few variables, whereas the rest of the variables have their loadings approaching zero, so that each variable could be associated to at most one component. A particular variable or group of variables having their respective loadings > 0.5 could be treated as the indicators of a source category or a principal component (Wilks 2006). Principal components with eigen values > 1.0 were retained in the results. Seven variables (WNA, PNA, 2-ring PAHs, 3-ring PAHs, 4-ring PAHs, Isoprenoids and Nicotine) were considered in the PCA resulting in three principal components (sources) explaining 82.1% of the total variance present in the NPOCs data-set. Table 3 presents the component loading matrix obtained from PCA.

## Results and discussion

### Influence of meteorological parameters

The annual mean values of meteorological parameters for the whole study period were found to be  $558 \pm 284$  m (PBL),  $22.0 \pm 7.2$  °C (T),  $4.2 \pm 9.0$  °C (Dp),  $35 \pm 12\%$  (RH),  $4.5 \pm$

$0.9$  knots (WS). The highest PBL ( $1083 \pm 55$  m) and T ( $31.5 \pm 0.3$  °C) was observed during the month of June, whilst the lowest values for the two parameters were observed during January (T:  $11.0 \pm 2.3$  °C) and December (PBL:  $214 \pm 43$  m). On the other hand, the maximum Dp ( $19.7 \pm 0.7$  °C) and RH ( $57 \pm 1\%$ ) was found during July, whilst the lowest values were observed during December (Dp:  $-8.7 \pm 3.1$  °C) and November (RH:  $22 \pm 7\%$ ). The maximum and minimum WS was found during the month of May ( $5.8 \pm 0.4$  knots) and August ( $2.8 \pm 0.4$ ), respectively. The observed seasonal trend in PBL (m) was spring (March-April-May (MAM);  $825 \pm 220$ ) > summer-monsoon (June-July-August (JJA);  $688 \pm 233$ ) > autumn (September-October-November (SON);  $419 \pm 128$ ) > winter (December-January-February (DJF);  $256 \pm 67$ ). The noticed seasonal trend in T (°C): JJA ( $29.0 \pm 1.8$ ) > MAM ( $25.5 \pm 4.7$ ) > SON ( $21.4 \pm 4.4$ ) > DJF ( $12.6 \pm 2.5$ ) and WS (knots) was MAM ( $5.7 \pm 0.5$ ) > DJF and SON ( $4.3 \pm 0.5$  and  $4.3 \pm 0.6$ ) > JJA ( $3.5 \pm 1.1$ ). Dp (°C) depicted the seasonal trend as: JJA ( $16.0 \pm 4.3$ ) > MAM ( $4.4 \pm 3.4$ ) > SON ( $1.1 \pm 8.9$ ) > DJF ( $-5.0 \pm 5.0$ ); and RH (%) showed following seasonal trend: JJA ( $49 \pm 15$ ) > DJF ( $32 \pm 13$ ) > MAM ( $29 \pm 11$ ) > SON ( $29 \pm 12$ ). Supplementary Fig. S1 shows the monthly modulations of meteorological variables. Higher PBL coupled with increase in T in spring and summer months results into increased volume for the diffusion of the pollutants, whereas during winters, low surface air temperature along with frequent episodes of radiation inversion leads to trapping of pollutants near to the ground level over subtropical or mid-latitude locations (Latini et al. 2002). Various studies have reported that an inverse relationship exists between PBL and pollutant concentration which means that boundary layer at greater heights favours more dilution of pollutants and lower pollution load near the ground level (Bringfelt 1971; Annand and Hudson 1981).

### Fine particulates (PM<sub>2.5</sub>) in the ambient air of Jammu

The annual mean concentration of fine particulates (PM<sub>2.5</sub>) during sampling period was found to be  $66.7 \pm 31.8$   $\mu\text{g m}^{-3}$ . In the ambient air of Jammu, the annual mean PM<sub>2.5</sub> concentration was higher than the permissible limit of NAAQS (annual mean:  $40$   $\mu\text{g m}^{-3}$ ) and WHO (annual mean:  $10$   $\mu\text{g m}^{-3}$ ). The highest 24-hourly mean  $160$   $\mu\text{g m}^{-3}$  (2015) and  $254$   $\mu\text{g m}^{-3}$  (2016) were found on Diwali day. Diwali festival is celebrated all over India and is one of the annual events when high particulate load (due to burning of fire crackers) is reported (Tandon et al. 2008). PM<sub>2.5</sub> concentration ( $\mu\text{g m}^{-3}$ ) represents the total mass of PM<sub>2.5</sub> present for mixing in the available volume of air, and any alteration in the PBL height will directly influence this mixing volume, which in return will affect the concentration of PM<sub>2.5</sub> in the ambient atmosphere. In order to have a better understanding of the variation in emission sources, it looks necessary to eliminate or

minimize the effect of monthly variation associated with PBL height. To achieve this, the scaled  $PM_{2.5}$  monthly mean concentrations were calculated by multiplying monthly mean  $PM_{2.5}$  concentration with dilution correction factor (DCF), defined as (Yadav et al. 2013a):

$$DCF_{month} = \frac{\text{Monthly average PBL}}{\text{Annual average PBL}}$$

Panel a of Fig. 2 shows the monthly mean  $PM_{2.5}$  concentration, and panel b of these figures shows corresponding scaled  $PM_{2.5}$  concentration. Fine particulate load was higher in winter months (Fig. 2a); however, after DCF scaling, the summer months show higher concentrations. High concentration of scaled  $PM_{2.5}$  in summer season illustrates the importance of DCF correction and also confirms higher source emissions during summers when compared to winters. The  $PM_{2.5}$  mass concentration showed strong seasonal variations: DJF ( $102 \pm 50.4 \mu\text{g m}^{-3}$ ) > SON; ( $84.0 \pm 28.9 \mu\text{g m}^{-3}$ ) > JJA; ( $47.6 \pm 9.4 \mu\text{g m}^{-3}$ ) > MAM; ( $32.6 \pm 11.4 \mu\text{g m}^{-3}$ ) (Fig. S2). The scaled  $PM_{2.5}$  concentrations in summer seasons show high source emissions. The scaled  $PM_{2.5}$  load was found to be high during spring and summer months (May and June) giving a strong indication of more active sources of emission during these months; however, high  $PM_{2.5}$  load is reported

during winter month can be attributed to lower PBL height (Pio et al. 2007).

### Monthly and seasonal variations in homologous series of n-alkanes

A total of 25 n-alkane homologues ( $C_{11}$ – $C_{35}$ ) were determined in fine particulates. The annual mean concentration of total n-alkanes (TNA) was equal to  $162 \pm 124 \text{ ng m}^{-3}$ . The monthly mean concentration of TNA (Fig. 3a) was maximum ( $518 \pm 338 \text{ ng m}^{-3}$ ) in June and minimum ( $53 \pm 52 \text{ ng m}^{-3}$ ) in August. To assess the effect of variations in PBL, the scaled TNA concentrations were calculated using DCF as discussed above in the case of  $PM_{2.5}$  concentration. When compared with monthly mean TNA concentrations (Fig. 3a), the observed monthly mean scaled TNA concentrations (Fig. 3b) were lower in winter months, whilst they showed similar pattern in summer months with maximum value in June. This corroborates that source emission rates were lesser in the winter season compared to summer. The annual average mass fraction of TNA in  $PM_{2.5}$  reached  $4008 \pm 3905 \text{ ppm}$  (Fig. 3c). It was maximum in June and minimum in February.

The seasonal mean TNA concentration in  $\text{ng m}^{-3}$  during different seasons followed the trend: JJA ( $344 \pm 336$ ) > MAM

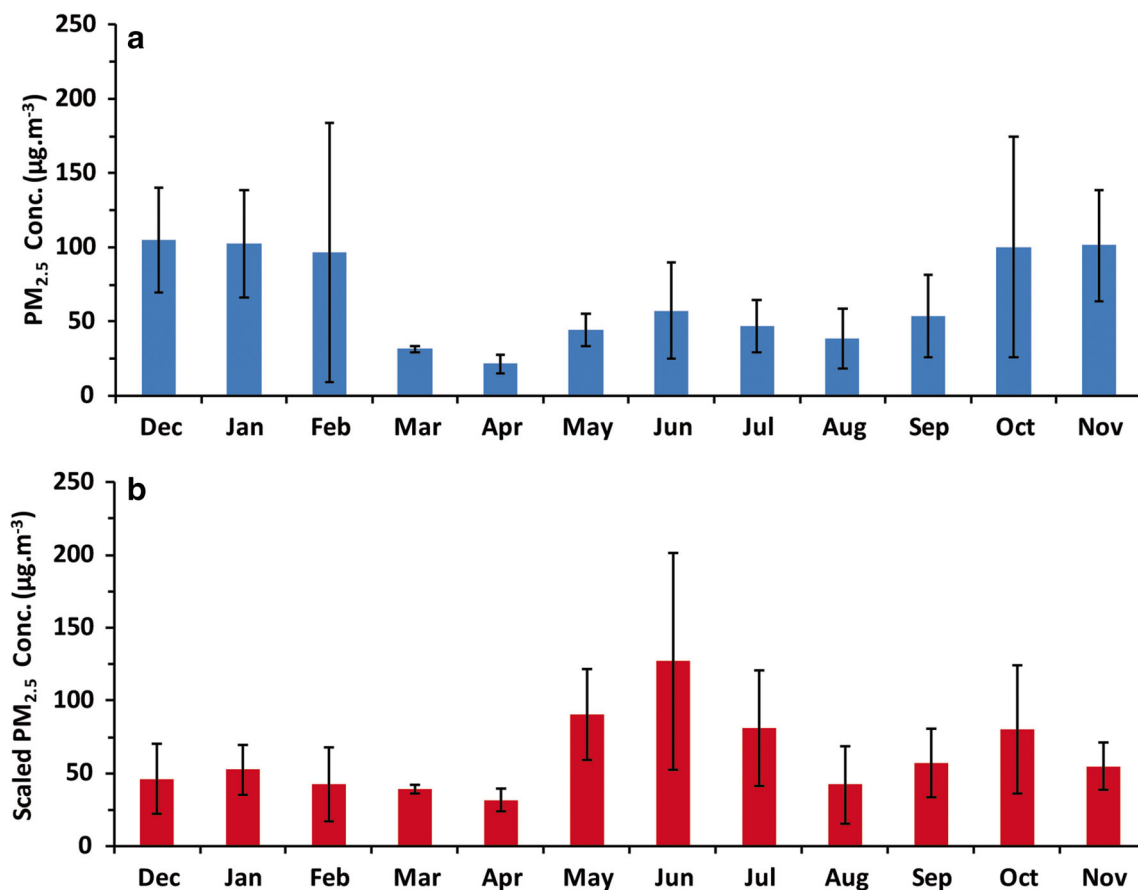
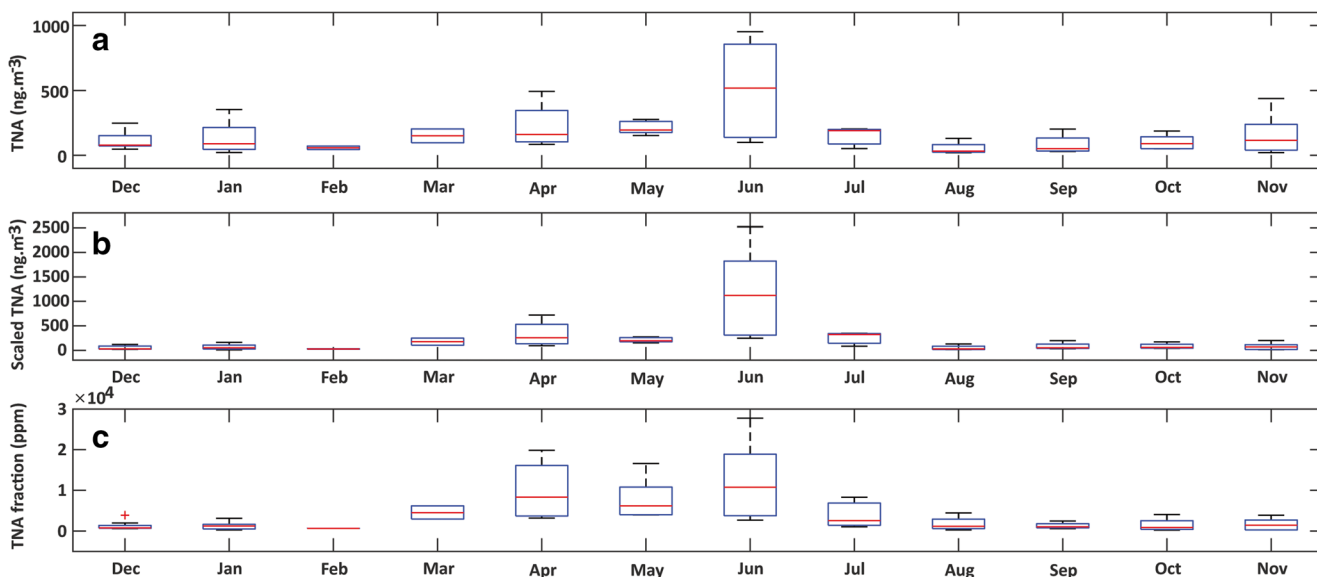


Fig. 2 Monthly mean mass concentration ( $\mu\text{g m}^{-3}$ ) (a) and scaled concentration ( $\mu\text{g m}^{-3}$ ) (b) of  $PM_{2.5}$





**Fig. 3** Monthly mean mass concentration ( $\text{ng m}^{-3}$ ) (a), scaled concentration ( $\text{ng m}^{-3}$ ) (b) and mass fraction (ppm) (c) of total n-alkane concentration (TNA)

$(206 \pm 113) > \text{DJF} (119 \pm 91) > \text{SON} (117 \pm 103)$  (Fig. S3). The seasonal mean scaled TNA concentration showed effect of PBL variation leading to lowest scaled TNA concentration in winter season (DJF). The fractional contribution of TNA to total fine particulate load in terms of TNA (ppm) was maximum in summer season and minimum in winter season:  $8306 \pm 8231 (\text{JJA}) > 8034 \pm 5777 (\text{MAM}) > 1292 \pm 2 (\text{SON}) > 1216 \pm 888 (\text{DJF})$ . N-alkanes can be broadly categorized as low molecular weight (LMW) for homologues with carbon number  $< 25$ , and high molecular weight (HMW) with carbon number  $C \geq 25$ . LMW n-alkanes are emitted from anthropogenic sources, such as incomplete combustion of fossil fuels, whilst HMW n-alkanes are generally contributed by plant waxes i.e. biogenic input. In this study, the annual mean of HMW/LMW was close to 1.9, indicating significant inputs from higher plants (Lyu et al. 2019).

**Total n-alkane-based diagnostic parameters**

Monthly average values of n-alkane associated diagnostic parameters (CPI,  $C_{\text{max}}$ , WNA%, PNA% and ACL) are given in Table 1. The annual mean CPI value was  $1.9 \pm 1.3$ , with maximum monthly average value of 4.7 during March and minimum of 0.5 during April. CPI values  $< 1$  are indicator of fossil fuel combustion and CPI  $> 1$  are from leaf waxes and other biogenic related inputs. In the present study, the annual average of CPI indicated mixed contributions from anthropogenic sources like fossil fuel related combustion with significant inputs from biogenic sources (Mancilla et al. 2016). Similar observations have been noticed in Delhi in year 2008 ( $1.8 \pm 0.7$ ) and 2009 ( $1.6 \pm 0.5$ ) (Yadav et al. 2013b), and also reported in Agra (CPI: 1.7) and Kanpur (CPI: 2.1) (Villalobos

et al. 2015). The maximum value 4.7 of CPI during the month of March (Fig. 4a) indicates that the biogenic derived emission sources were more active during this month. The sudden fall of CPI to 0.5 indicates heavy load of petrogenic emissions, which could be due to the increased fossil fuel combustion because of increase in religious tourists to Shri Mata Vaishno Devi Shrine (SMVDS) located in Katra. The religious tourists from all over India and abroad reach Katra through Jammu by road/rail/air and leads to increase in fossil fuel utilization in the region. The seasonal CPI variations were noted to be  $2.2 \pm 3.0 (\text{SON}) > 1.9 \pm 3.0 (\text{MAM}) > 1.7 \pm 1.2 (\text{DJF}) > 0.9 \pm 1.4 (\text{JJA})$ . The value of 0.9 reported in summer again overlaps with the heavy tourist load to SMVDS during this peak season. The CPI value around 2.2 during autumn shows biogenic influence from pollen emissions and suspension of crystalline epicuticular waxes caused by wind action and re-suspension of garden/road dust (Yadav et al. 2013a). The mean CPI in Jammu is close to that reported from Srinagar (CPI:  $1.7 \pm 0.6$ ) but the seasonal characteristics of CPI in Jammu are entirely different from that reported in Srinagar, where low CPI values in autumn to winter season with minimum CPI ( $0.9 \pm 0.2$ ) in November month and high CPI values in JJA were noticed (Huma et al. 2016).

The  $C_{\text{max}}$  value, a measure of the most abundant n-alkane in the n-alkane series ( $C_{11}\text{-}C_{35}$ ), indicates the probable contribution of n-alkanes from different sources to  $\text{PM}_{2.5}$  aerosol load. The most predominant carbon number among the homologue series of n-alkanes during the sampling period occurred at  $C_{29}$  (Table 2).  $C_{\text{max}}$  at  $C_{29}$  is an indicator of n-alkanes arising from road dust with mixed accumulation of emissions from vehicular and industrial sector along with plant litter mix deposited on the surface and has been previously reported in

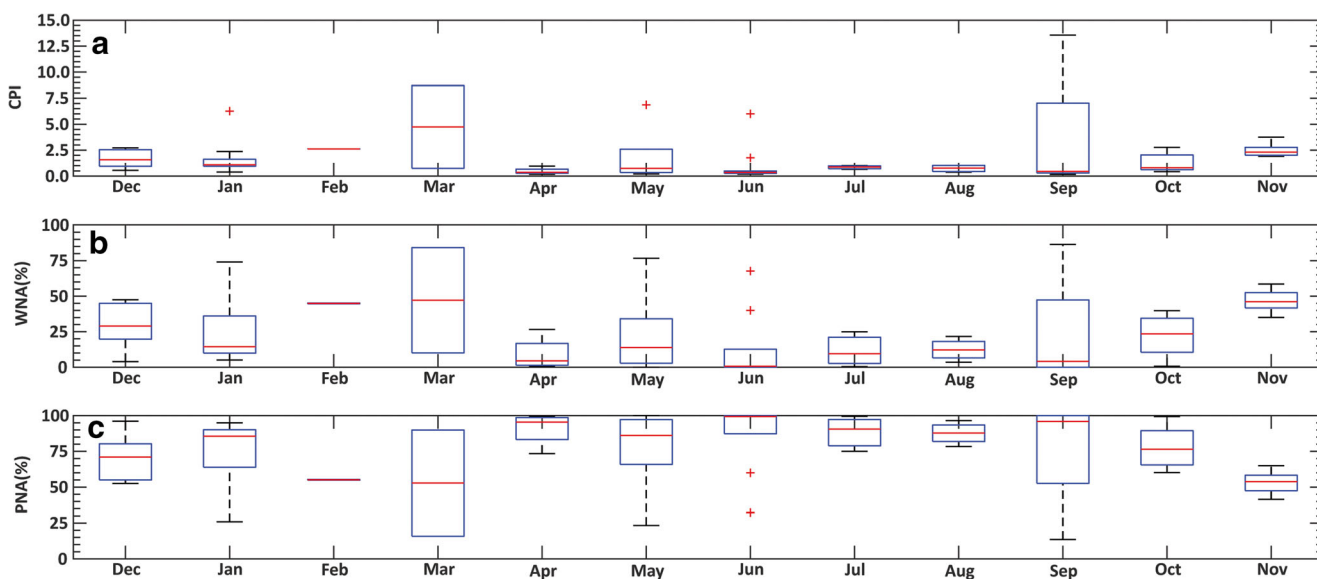


**Fig. 4** Monthly mean values of Carbon Preference Index (CPI) (a), percentage contribution of WNA (wax n-alkane) (b), and percentage contribution of PNA (petrogenic n-alkane) (c)

Delhi (Chowdhury et al. 2007; Yadav et al. 2013a; Wan et al. 2016). The  $C_{max}$  values for different seasons was as follows: autumn ( $C_{29}$ ,  $C_{27}$ ), winter ( $C_{29}$ ,  $C_{25}$ ), spring ( $C_{28}$ ,  $C_{30}$ ) and summer ( $C_{30}$ ,  $C_{28}$ ). In this study, mostly the  $C_{max}$  value was at  $C \geq 27$ , which indicates n-alkane emissions originating from epicuticular waxes, whereas in the month of December ( $C_{20}$ ), January ( $C_{20}$  and  $C_{25}$ ) and April ( $C_{17}$ ,  $C_{24}$ )  $C_{max}$  remained  $< C_{27}$ , which indicates influence of petrogenic contributions.

The Wax n-alkanes contribution to total n-alkanes is indicated as WNA%. It is a marker for biogenic sources, particularly from epicuticular surface of plant leaves (Gupta et al. 2017). The annual mean WNA% for the homologue series of n-alkanes was  $25.4 \pm 14.0\%$ . The maximum ( $47.1 \pm 52.4\%$ ) and minimum ( $9.0 \pm 12.0\%$ ) values occurred during the month of March and April respectively (Fig. 4b), whereas

petrogenic contribution (PNA%) was found to be  $74.6 \pm 14.0\%$  (annual mean) with maximum ( $91.0 \pm 12.0\%$ ) in April and minimum ( $52.9 \pm 52.4\%$ ) in March (Fig. 4c). The seasonal variations in WNA% showed maximum biogenic contribution in autumn and minimum in summer season:  $30.7 \pm 23.6\%$  (SON)  $> 26.6 \pm 17.8\%$  (DJF)  $> 22.2 \pm 30.0\%$  (MAM)  $> 12.4 \pm 18.2\%$  (JJA). The contribution of petrogenic (PNA%) sources (vehicular and industrial) to total n-alkanes, was found to be:  $87.7 \pm 18.2\%$  (JJA)  $> 77.8 \pm 30.0\%$  (MAM)  $> 73.4 \pm 17.8\%$  (DJF)  $> 69.3 \pm 23.6\%$  (SON).

The average chain length (ACL) is an indicator of emissions of aliphatic hydrocarbons from plants. Based on the prevalence of odd carbon numbered higher plant n-alkanes, it represents the average number of carbon atoms present per molecule (Yadav et al. 2013a). The mean ACL value in this study was  $27.7 \pm 1.3$ . Seasonal variations in ACL values were  $28.7 \pm 1.7$  (MAM),  $28.4 \pm 2.9$  (JJA),  $27.9 \pm 2.4$  (SON) and,  $26.7 \pm 2.0$  (DJF). The ACL values reported here are much lesser than those found in Delhi by (Yadav et al. 2013a).

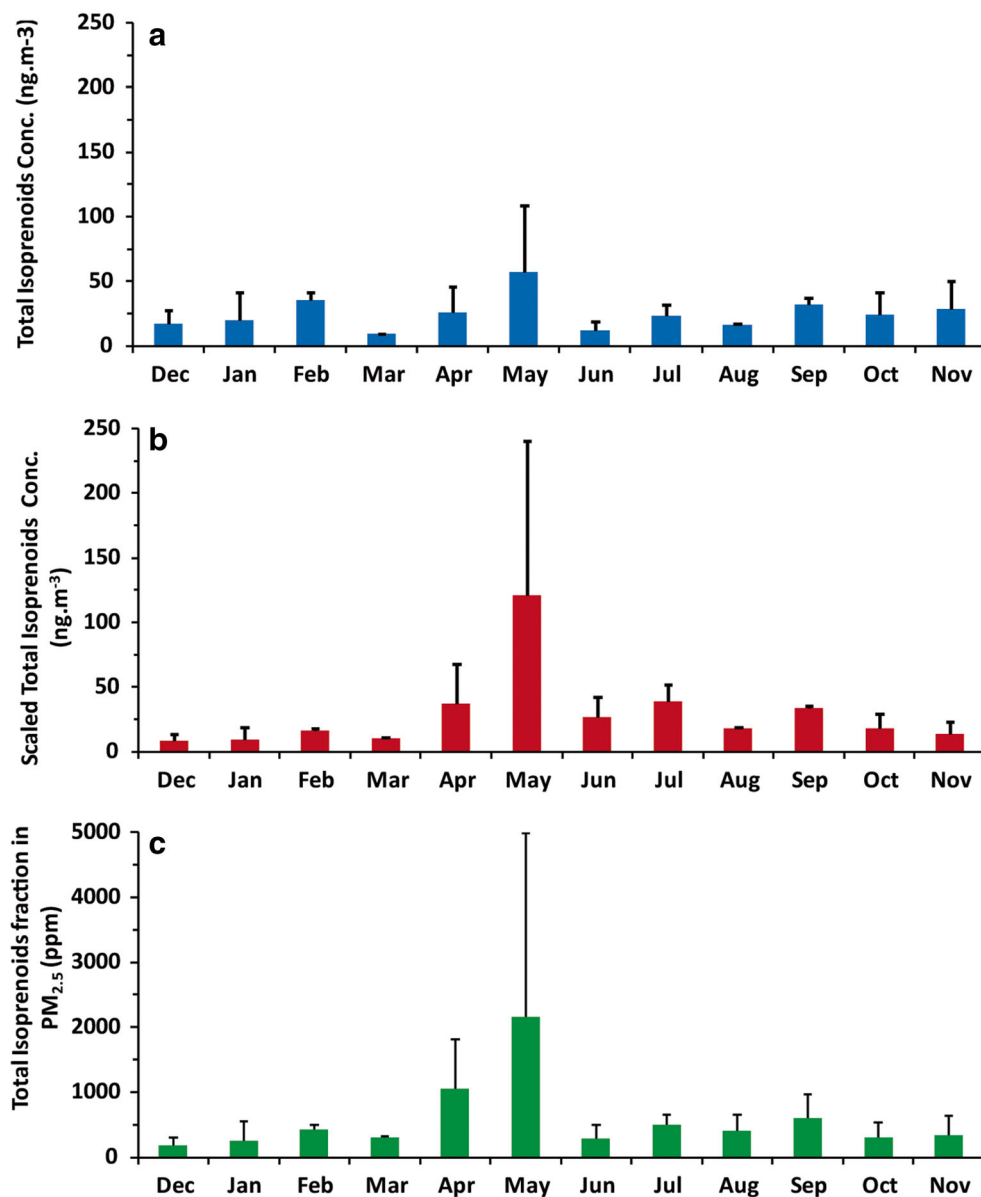
**Table 2** Monthly mean values of TNA-based diagnostic parameters used for source characterization

Month	CPI	$C_{max}$	WNA%	PNA%	ACL
Dec	$1.6 \pm 0.8$	25, 29	$29.9 \pm 15.5$	$70.1 \pm 15.5$	$27.0 \pm 1.0$
Jan	$1.5 \pm 1.4$	20, 25, 31	$22.3 \pm 18.8$	$77.7 \pm 18.8$	$26.5 \pm 2.6$
Feb	$2.6 \pm 0.0$	29.00	$44.9 \pm 0.4$	$55.1 \pm 0.4$	$27.3 \pm 0.2$
Mar	$4.7 \pm 5.6$	29.00	$47.1 \pm 52.4$	$52.9 \pm 52.4$	$28.7 \pm 0.6$
Apr	$0.5 \pm 0.3$	17, 24, 30	$9.0 \pm 12.0$	$91.0 \pm 12.0$	$28.5 \pm 1.1$
May	$1.9 \pm 2.8$	28, 33, 34	$22.8 \pm 31.1$	$77.2 \pm 31.1$	$28.9 \pm 2.4$
Jun	$1.0 \pm 1.8$	28, 30	$12.6 \pm 23.1$	$87.4 \pm 23.1$	$30.0 \pm 2.2$
Jul	$0.8 \pm 0.2$	29.00	$11.6 \pm 12.4$	$88.4 \pm 12.4$	$27.6 \pm 2.4$
Aug	$0.7 \pm 0.3$	28.00	$12.3 \pm 7.7$	$87.7 \pm 7.7$	$25.0 \pm 1.4$
Sep	$3.7 \pm 6.6$	28, 29	$23.7 \pm 42.0$	$76.3 \pm 42.0$	$26.9 \pm 1.3$
Oct	$1.3 \pm 0.9$	27, 33, 34	$22.2 \pm 14.9$	$77.8 \pm 14.9$	$27.9 \pm 3.2$
Nov	$2.5 \pm 0.7$	27, 29, 31	$46.7 \pm 8.2$	$53.3 \pm 8.2$	$28.5 \pm 1.8$

### Monthly and seasonal variations in isoprenoid hydrocarbons

Pristane (Pr; C-19 isoprenoid; 2,6,10,14-tetramethylpentadecane), phytane (Ph; C-20 isoprenoid; 2,6,10,14-tetramethylhexadecane) and farnesane (Fr; C-15 isoprenoid; 2,6,10-trimethyldodecane) are the three important isoprenoid hydrocarbons detected in the  $PM_{2.5}$  samples. The presence of these isoprenoid hydrocarbons indicates contribution from fossil fuel burning (Yadav et al. 2013b). Figure 5 shows monthly average concentration of total isoprenoids (panel a), scaled total isoprenoids (panel b) and mass fraction of total isoprenoids in  $PM_{2.5}$  (panel c). Monthly

**Fig. 5** Monthly mean mass concentration ( $\text{ng m}^{-3}$ ) (a), scaled concentration ( $\text{ng m}^{-3}$ ) (b) and mass fraction (ppm) (c) of total isoprenoids



mean concentration of total isoprenoids (pristane+phytane+farnesane) ranged from 10 to 57  $\text{ng m}^{-3}$  with an annual average value of  $26 \pm 12 \text{ ng m}^{-3}$ . The maximum and minimum concentrations for total isoprenoids were observed in May and March, respectively. The minimum concentration of isoprenoids in March indicates minimum vehicular contributions and this is analogous to the above observation where CPI value of  $4.7 \pm 5.6$  shows dominance of biogenic emissions in the month of March. The annual mean mass fraction of total isoprenoids in  $\text{PM}_{2.5}$  was  $580 \pm 547 \text{ ppm}$  ranging from  $257 \pm 298 \text{ ppm}$  in January to  $2163 \pm 2833 \text{ ppm}$  during May. A well-established seasonal variation was also observed in the mean values of total isoprenoids:  $31 \pm 24 \text{ ng m}^{-3}$  (spring; MAM)  $> 28 \pm 4 \text{ ng m}^{-3}$  (autumn; SON)  $> 24 \text{ ng m}^{-3} \pm 10$  (winter; DJF)  $> 17 \pm 6 \text{ ng m}^{-3}$  (summer; JJA). Phytane is

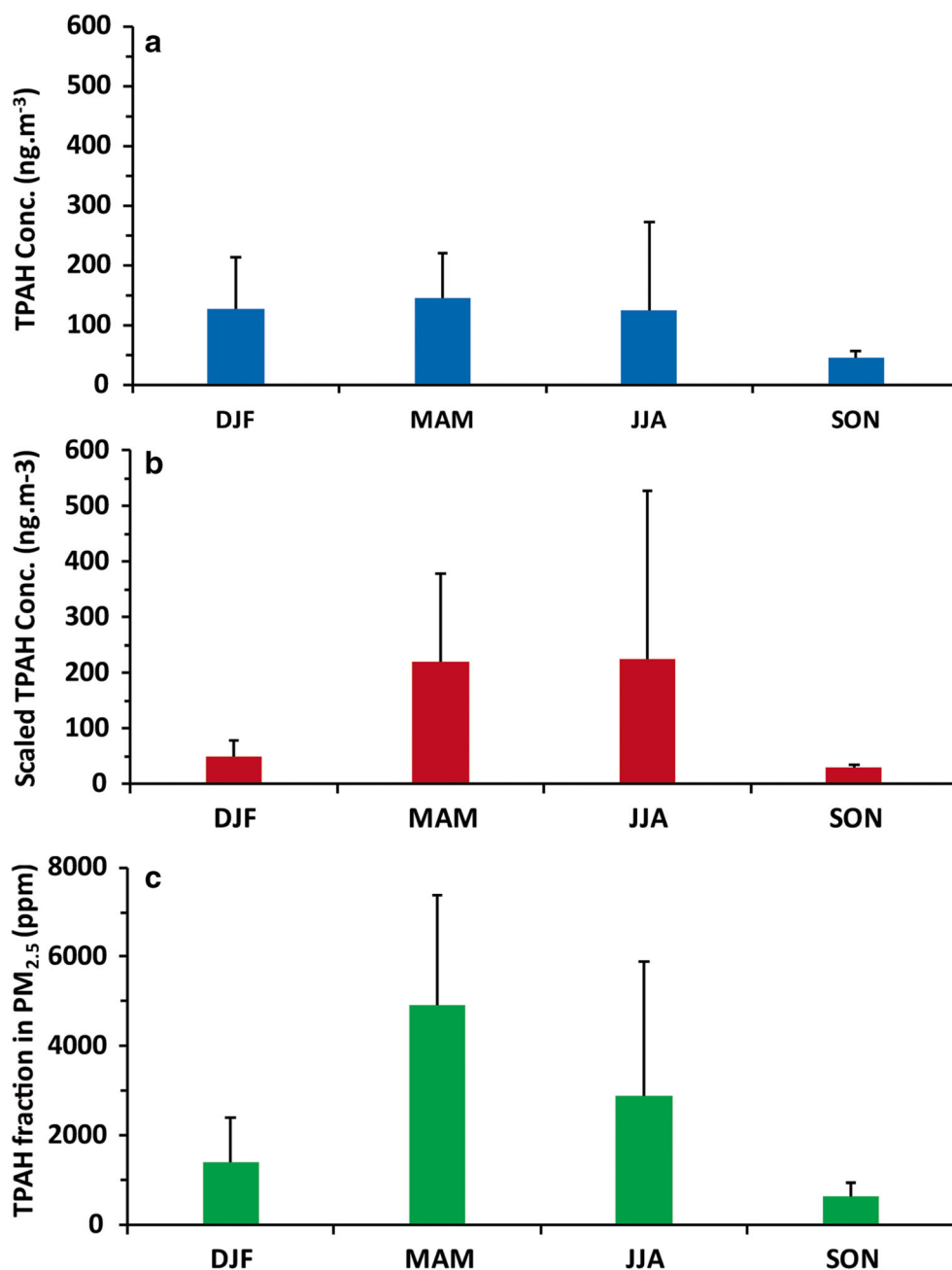
rarely found in biological materials and thus pristane/phytane (Pr/Ph) ratio can be used to differentiate between biogenic and petrogenic (petroleum) related emissions, with Pr/Ph values  $> 1$  for biogenic input and  $< 1$  as petrogenic or hydrocarbon-related emission of isoprenoids (Alves et al. 2014; Křůmal et al. 2017). The annual mean value of Pr/Ph was found to be 1, suggesting mixed emissions of  $\text{PM}_{2.5}$  aerosol-associated hydrocarbons. The seasonal variations in the Pr/Ph values was JJA (1.0)  $>$  DJF (0.9)  $>$  MAM (0.7)  $>$  SON (0.7). The observed seasonal mean values of Pr/Ph in this study remained  $\leq 1$ , showing dominance of petrogenic contributions to isoprenoid hydrocarbons in the region. The Pr/Ph ratio of  $\leq 1$  has also been observed from other urban locations and can be compared to the reported values in this study (Supplementary Table S1).

## Monthly and seasonal variations in polycyclic aromatic hydrocarbons

PM<sub>2.5</sub> aerosol samples were analysed for 16 PAHs, and overall predominance of 10 PAHs was noticed: naphthalene (NAP), acenaphthylene (ACY), acenaphthene (ACE), fluorene (FL), phenanthrene (PHE), anthracene (ANT), fluoranthene (FLU), pyrene (PYR), chrysene (CHY), and benzo[k]fluoranthene (BkF). The monthly mean  $\sum$ PAH (TPAH) concentration ranged from  $35 \pm 34 \text{ ng m}^{-3}$  in September to  $295 \pm 254 \text{ ng m}^{-3}$  during June respectively with annual mean value of  $111 \pm 90 \text{ ng m}^{-3}$ . The TPAH concentration followed an increasing trend from March to June, and

June onwards there was a sharp decrease in the TPAH concentration. Despite high PBL ( $1083 \pm 55 \text{ mts}$ ) in the month of June, maximum TPAH concentration ( $295 \pm 254 \text{ ng m}^{-3}$ ) indicates enhanced emissions of particulate bound TPAHs during this month. This observation coincides with highest number of yatri visiting SMVDS in the month of June and the TPAH concentration decreases as the number of these yatri decreases from summers to winters. The influx of yatri in large number could be one major reason of combustion related emissions in the region. The seasonal variation in the mean TPAHs followed the pattern: MAM ( $146 \pm 74 \text{ ng m}^{-3}$ ) > DJF ( $127 \pm 87 \text{ ng m}^{-3}$ ) > JJA ( $125 \pm 147 \text{ ng m}^{-3}$ ) > SON ( $45 \pm 13 \text{ ng m}^{-3}$ ) (Fig. 6a). The scaled seasonal mean TPAH

**Fig. 6** Seasonal mean mass concentration ( $\text{ng m}^{-3}$ ) (a), scaled concentration ( $\text{ng m}^{-3}$ ) (b) and mass fraction (ppm) (c) of total PAH concentration

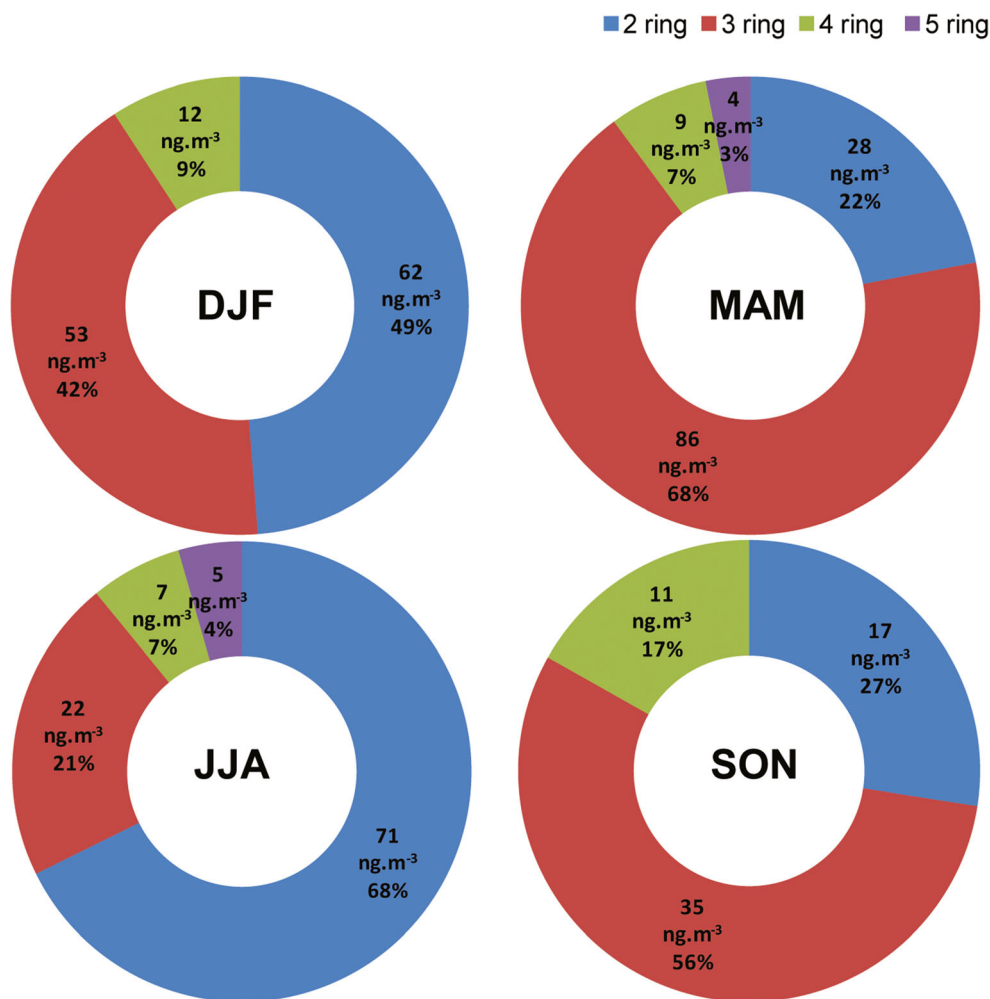


concentrations were calculated after scaling to respective PBL heights (m) (Fig. 6b). The maximum scaled seasonal mean in JJA again confirms high source emissions in this season with maximum contribution in June. High TPAH concentrations in winters with  $226 \pm 115 \text{ ng m}^{-3}$  during February show the combined effect of decreasing volatility of PAHs with temperature (Mancilla et al. 2016), lower PBL and increased biomass burning for heating purpose during this period (Yadav et al. 2013b). Further, in winters the value of  $[(\text{FLU} / (\text{FLU} + \text{PYR}))]$  was found to be 1.18 indicating combustion of grass, wood and coal as the major source of emissions during this time. The ratio of  $[\text{Flu} / (\text{Flu} + \text{Pyr})]$ :  $> 0.5$  indicates grass, wood or coal combustion,  $0.4\text{--}0.5$  indicates fossil fuel combustion, and values  $< 0.5$  indicate petrogenic origin of PAHs. A similar study by Vicente et al. (2011) reported values for  $\text{Flu}/(\text{Flu} + \text{Pyr})$  within  $0.53\text{--}0.86$  suggesting emission of  $\text{PM}_{2.5}$  bound PAHs from biomass burning. These diagnostic ratios also depicted seasonal variations, with  $[(\text{Flu} / (\text{Flu} + \text{Pyr}))]$  values around 1.06 and 2.64 in winters and autumn season again indicating influence of coal, grass and wood combustion as the main sources of  $\text{PM}_{2.5}$  bound PAHs into the atmosphere. The annual mean mass fraction of TPAHs stood at  $2466 \pm$

$2413 \text{ ppm}$  and the monthly mean mass fraction varied from  $400 \pm 306 \text{ ppm}$  in October to  $7019 \pm 7494 \text{ ppm}$  in May. The variations in mass fraction also followed a seasonal pattern with maximum contribution in spring-summer season:  $\text{MAM} (4914 \pm 2457 \text{ ppm}) > \text{JJA} (2899 \pm 2994 \text{ ppm}) > \text{DJF} (1394 \pm 1024) > \text{SON} (658 \pm 276)$  (Fig. 6c).

The annual percentage contribution of different PAHs was 2 rings (45%), 3 rings (43%), 4 rings (10%) and 5 rings (2%). A clear dominance of LMW PAHs (with 2 and 3 aromatic rings) in this study denotes dominance of biomass burning over fossil fuel burning activities. HMW (with 4 and 5 aromatic rings) were also spotted but toxic PAHs like BkF were very rarely found in the samples. The contribution of 2-ring PAHs was minimum in MAM (22%), succeeded by SON (27%), DJF (49%) and then JJA (68%), whereas the contribution of 3-ring PAHs was 68% for MAM, 56% for SON, 42% for DJF and 21% for JJA (Fig. 7). The 2-ring PAHs NAP is mostly found in vapour phase and is prone to fast photo-degradation. Dominance of NAP shows emissions from some local source and this observation requires further investigation. The predominant 3-ring PAHs (ACY, ACE, FLU, PHE, ANT) suggesting substantial contribution from low

Fig. 7 Ring-based distribution of total PAHs in different seasons



temperature pyrolysis processes (like biomass combustion), incineration as the major PAH source (Huma et al. 2016; Roy et al. 2019). The 4-ring species indicating coal combustion related emissions accounted for about 9% for winter, 7% for spring and summer and 17% during autumn. BkF (with 5-aromatic rings) a marker for emissions arising from vehicular exhaust was detected only during spring and summer, that too in rare quantities (3% and 4%, respectively). The [ANT/(ANT+PHE)] is also a good indicator of petrogenic versus pyrogenic ratio: values < 0.1 indicate petrogenic emissions and > 0.1 indicate pyrogenic input (Yadav et al. 2013b; Zhang et al. 2018b). The mean [ANT/(ANT + PHE)] ratio was found to be higher than 0.1, with values around 0.20 and 0.50 in JJA (summers) and SON (autumn) respectively, indicating contributions of pyrogenic (combustion) derived sources of PAHs. The TPAH concentrations reported in the present study were closer to those reported by Kalaiarasan et al. (2018) at a traffic site in Mangalore, Karnataka (109 ng m<sup>-3</sup>). Dubey et al. (2015) reported the TPAH concentration of about 880.8 ± 2.7 ng m<sup>-3</sup>, approximately eight times higher as compared to the current study. On the other hand, Masih et al. (2019) reported quite low values (29.36 ± 0.44 ng m<sup>-3</sup>) in Mumbai. Our results in terms of dominance of LMW PAHs differed from previous studies performed using the same thermal desorption method. Yadav et al. (2013b) reported the presence of ≥ 5 ring PAHs in PM<sub>10</sub> samples collected from Delhi, whilst Huma et al. (2016) noted the dominance of 3- and 4-ring PAHs over 5 and 6 ring PAHs in the TSPM samples collected in Srinagar, Jammu & Kashmir.

### Nicotine, a source marker for environmental tobacco smoke

Nicotine was detected in almost all the months with mass fractions ranging from 10,121 ± 1471 ppm in April to 2311 ± 325 ppm in February. The monthly mean concentration (ng m<sup>-3</sup>) and scaled monthly mean concentration (ng m<sup>-3</sup>) of nicotine are plotted in panel a and panel b, whereas mass fraction of nicotine (ppm) in PM<sub>2.5</sub> is shown in panel c of Fig. 8. The monthly mean concentration of nicotine was highest (345 ± 297 ng m<sup>-3</sup>) in December and lowest (111.80 ± 94.41 ng m<sup>-3</sup>) in June, with annual mean value of 227 ± 69 ng m<sup>-3</sup>. The scaled nicotine concentration was maximum in the month of March, April and May, showing increased source emissions in these months. The nicotine concentration observed in Jammu is lower than the annual mean concentration of 388 ± 307 ng m<sup>-3</sup> reported by Huma et al. (2016), in Srinagar and a mean concentration of around 448 ± 260 ng m<sup>-3</sup> reported by Yadav et al. (2014) in the ambient atmosphere of Delhi. In another study by Khedidji et al. (2017), even lower nicotine concentrations ranging from 9.6 to 137 ng m<sup>-3</sup>

were reported in Bouira Province, Algeria. Van Drooge et al. (2018) attributed 38 ng m<sup>-3</sup> of nicotine concentration in Barcelona, Spain, to human-related activities, particularly cigarette smoking. The higher concentration of nicotine in December (winter) than summer (June) can be attributed to lower photo-degradation and increased input sources, particularly through anthropogenic activities (Huma et al. 2016). The seasonal variations in the nicotine concentration showed a similar pattern in other seasons except summers: winter (294 ± 244 ng m<sup>-3</sup>) > autumn (264 ± 169 ng m<sup>-3</sup>) > spring (243 ± 80 ng m<sup>-3</sup>) > summer (140 ± 100 ng m<sup>-3</sup>). However, the mass fraction of nicotine was quite high in spring, when compared to other seasons: spring (8017 ± 2655 ppm) > autumn (3923 ± 3386 ppm) > winter (3619 ± 3384 ppm) > summer (3173 ± 2514 ppm).

### Temporal variations in other organic markers

Among other organic markers, levoglucosan was detected in most of the samples, whilst other markers like isoquinoline, methylphenanthrene, retene and dehydroabietic acid were only sporadically noticed. The presence of levoglucosan in most of the months confirms the contribution from biomass burning (Nirmalkar et al. 2015; Mancilla et al. 2016). Strong seasonal variations in levoglucosan with dominance in spring and winter season suggest high emissions from biomass burning in these months in the form of residential heating, cooking and garden waste burning (Herlekar et al. 2012). The rare presence of source markers viz. retene and dehydroabietic acid indicate lower impact from coniferous wood combustion. The sampling area is as such devoid of any coniferous vegetation in the vicinity. The contributions from coniferous wood combustion may be attributed to emissions through wind assisted long-range transport. In addition, there is a crematorium near to the sampling site, where cremation takes place frequently. However, the sampling site is in upwind direction to this graveyard but still sometimes excessive emission may lead to persistence of burning markers in the atmosphere, affecting the sampling site. Methylphenanthrene was detected only in summers, which is consistent with previous findings where same trend of contributions from unburned fossil fuel (i.e. evaporative fuel losses from roadway etc.) due to higher ambient temperature were reported (Li et al. 2009). Isoquinoline, an ETS constituent, was detected in winter season; however, no direct correlation between nicotine and isoquinoline could be traced to confirm its emission from cigarette smoke.

### Source identification through principal component analysis

Principal component analysis applied on the data-set of the concentrations of various PM<sub>2.5</sub> associated NPOCs helped in the identification of their major sources over the study area

**Fig. 8** Monthly mean mass concentration ( $\text{ng m}^{-3}$ ) (a), scaled concentration ( $\text{ng m}^{-3}$ ) (b) and mass fraction (ppm) (c) of nicotine

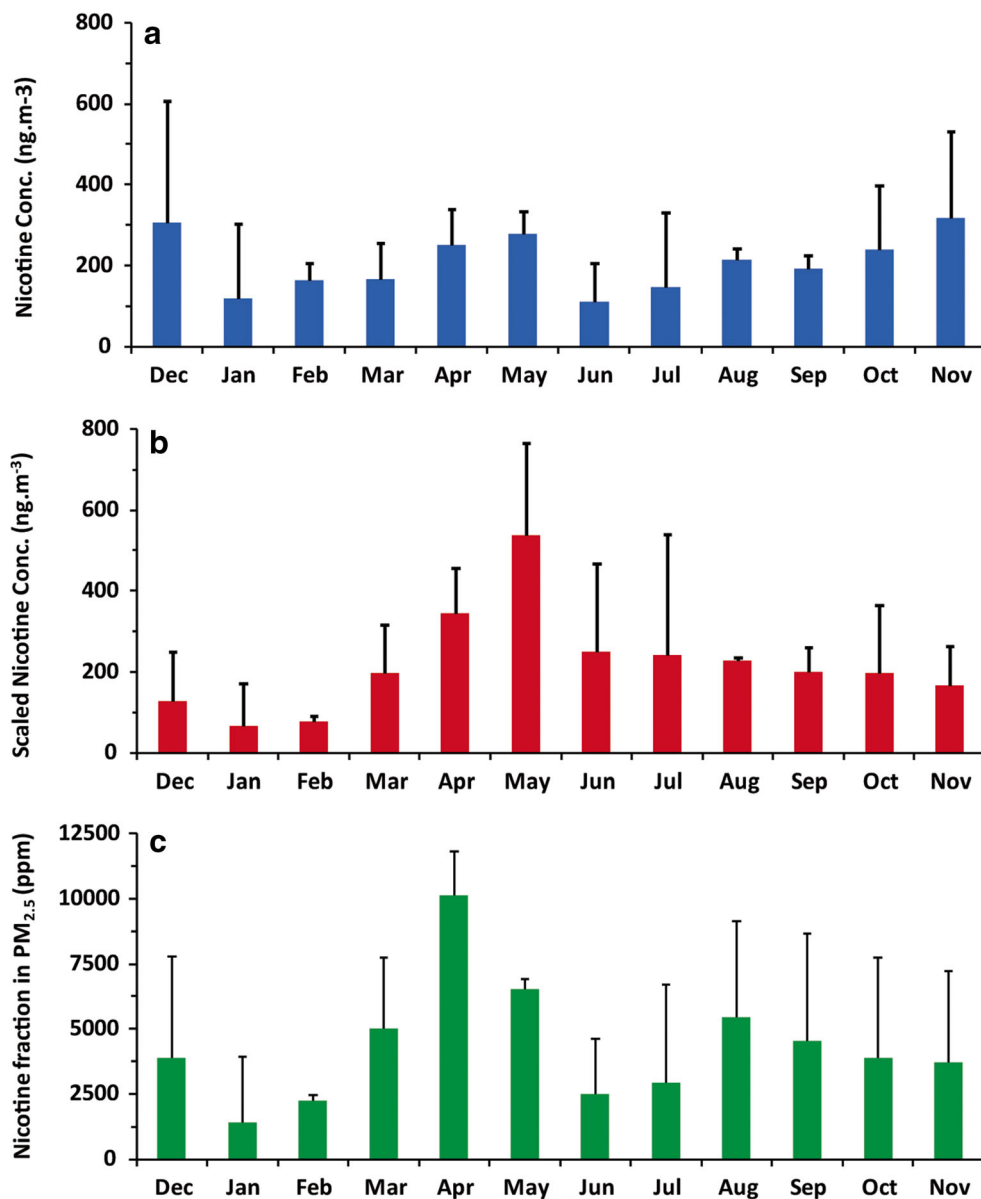


(Table 3). At the urban location Jammu, three main sources were revealed: (a) the first principal component (PC1) having higher loadings for PNA (0.85), and 2-ring PAHs (0.88) that explained ~30% of the total variance plausibly traced to the emissions from gasoline and diesel engines as well as evaporative losses from the nearby depots of refined petroleum products (Alves et al. 2019, 2017; Li et al. 2019; Masih et al. 2019; Sarti et al. 2017); (b) second principal component (PC2) which also explained ~30% of total variance with higher loadings for 3-ring PAHs (0.85), and isoprenoids (0.91), signifies the emissions from coal and wood burning as the second major source of aerosol-associated NPOCs (Alves et al. 2014; Huma et al. 2016; Křůmal et al. 2017; Roy et al. 2019; Yadav et al. 2013b); and (c) the third principal component (PC3) was having higher loadings of WNA (0.86), and 4-ring PAHs (0.72) and explained ~22% of total variance

**Table 3** Varimax rotated principal component loadings of  $\text{PM}_{2.5}$  associated NPOCs

Source tracers	PC1	PC2	PC3
WNA	0.35	-0.01	<i>0.86</i>
PNA	<i>0.85</i>	0.03	0.21
Two ring PAHs	<i>0.88</i>	0.12	0.03
Three ring PAHs	0.13	<i>0.85</i>	-0.03
Four ring PAHs	-0.21	-0.57	<i>0.72</i>
Isoprenoids	-0.10	<i>0.91</i>	-0.09
Nicotine	-0.63	0.44	0.49
Eigen values	2.09	2.09	1.56
% of variance explained	29.93	29.92	22.25

Variables with loadings > 0.5 (shown in italics) are used as an indicator of a source category

present in NPOCs data-set could be sourced to the re-suspension of decomposed litter/biomass and agricultural refuse burning leftovers from the nearby fields (Abas and Simoneit 1996; Javed et al. 2019; Lyu et al. 2019; Pio et al. 2001; Zhang et al. 2018a, b).

## Conclusions

The annual mean concentration of PM<sub>2.5</sub> during the sampling period was found higher than the permissible limit of India's NAAQS and WHO guidelines. As expected, the maximum 24 hourly mean was noticed on the Diwali day. Though the annual mean concentration for PM<sub>2.5</sub> and associated organic species was lesser than the concentrations reported from pollution hotspots like Delhi, the seasonal variations were similar with high source contributions in summer season. The pattern of seasonal variations observed in the concentration of organic species at Jammu was different from the reported concentrations from Srinagar. The high concentrations of NPOCs in June were possibly due to high source emissions and dry conditions in this month, as monsoon arrives in the first week of July in this part of the NWHR. The n-alkane-based diagnostic parameters indicated mixed contributions of NPOCs from anthropogenic sources like fossil fuel-related combustion with significant inputs from biogenic sources. These diagnostic parameters further showed high influence of petrogenic contribution in summer (monsoon) months. The presence of quantifiable isoprenoid hydrocarbons, as tracers for vehicular emissions confirmed this observation. Total PAHs concentration also followed an increasing trend from March to June, and June onwards a sharp decrease was observed. This coincides with the highest number of yatis visiting nearby Shri Mata Vaishno Devi Shrine in these months. The large influx of yatis in summer months could be a major reason of combustion-related emissions in the region. The concentration of ETS marker nicotine was found lower than as previously reported in Srinagar and Delhi. The higher concentration of nicotine observed in winter months than summers can be attributed to lower air temperature with lower photo-degradation settings. The presence and dominance of LMW PAHs (with 2 and 3 aromatic rings) in this study is interesting and calls for more comprehensive investigations. The toxic PAHs were rare in the ambient atmosphere of Jammu. PAH-based diagnostic parameters suggested substantial contribution from low temperature pyrolysis processes like biomass/crop-residue burning, wood and coal fire in the region. Specific wood burning markers like levoglucosan, retene and dehydroabietic acid also supported this finding. As this region of the North-Western Himalaya has variable altitudinal and land-use settings, this investigation may further be extended to the diverse locations to understand the dynamics in sources and processes modulating aerosol

characteristics. This will further help in understanding the overall aerosol chemistry and its implications on the regional climate of the North-Western Himalayan Region.

**Acknowledgements** We thank NOAA-ARL for providing meteorological data. We are thankful to Prof. Arun K. Attri for providing access to his laboratory facility in School of Environmental Sciences, Jawaharlal Nehru University, New Delhi. Prof. Arun K. Attri and Dr. Ajay Kumar have been acknowledged for TD-GC-MS analysis at Advanced Instrumentation Research Facility at Jawaharlal Nehru University. Authors thank anonymous reviewers for their contribution in improving the manuscript.

**Funding information** This research was funded by University Grants Commission, India, in the form of Major Research Project no. MRP-MAJOR-ENVI-2013-30069 vide file no. 43-332/2014.

## References

- Abas M, Simoneit BRT (1996) Composition of extractable organic matter of air particles from Malaysia: initial study. *Atmos Environ* 30: 2779–2793
- Alves C, Nunes T, Vicente A et al (2014) Speciation of organic compounds in aerosols from urban background sites in the winter season. *Atmos Res* 150:57–68. <https://doi.org/10.1016/j.atmosres.2014.07.012>
- Alves CA, Vicente AM, Custódio D et al (2017) Polycyclic aromatic hydrocarbons and their derivatives (nitro-PAHs, oxygenated PAHs, and azaarenes) in PM 2.5 from Southern European cities. *Sci Total Environ* 595:494–504. <https://doi.org/10.1016/j.scitotenv.2017.03.256>
- Alves CA, Vicente ED, Evtyugina M et al (2019) Gaseous and speciated particulate emissions from the open burning of wastes from tree pruning. *Atmos Res* 226:110–121. <https://doi.org/10.1016/j.atmosres.2019.04.014>
- Andreae MO, Gelencs A, Box PO, Veszpr H (2006) Andreae\_ACP2006.pdf. *Atmos Chem Phys*:3131–3148. <https://doi.org/10.5194/acpd-6-3419-2006>
- Annand WJ, Hudson AM (1981) Meteorological effects on smoke and sulphur dioxide concentrations in the manchester area. *Atmos Environ* 15:799–806
- Bond TC, Doherty SJ, Fahey DW et al (2013) Bounding the role of black carbon in the climate system: a scientific assessment. *J Geophys Res Atmos* 118:5380–5552. <https://doi.org/10.1002/jgrd.50171>
- Bray E, Evans E (1961) Distribution of n-paraffins as a clue to recognition of source beds. *Geochim et Cosmochim Acta* 22:2–15
- Bringfelt B (1971) Important factors for the sulphur dioxide concentration in Central Stockholm. *Atmos Environ* 5:949–972
- Carrico CM, Bergin MH, Shrestha AB et al (2003) The importance of carbon and mineral dust to seasonal aerosol properties in the Nepal Himalaya. *Atmos Environ* 37:2811–2824. [https://doi.org/10.1016/S1352-2310\(03\)00197-3](https://doi.org/10.1016/S1352-2310(03)00197-3)
- Chalbot M, Vei I, Lianou M et al (2012) Environmental tobacco smoke aerosol in non-smoking households of patients with chronic respiratory diseases. *Atmos Environ* 62:82–88. <https://doi.org/10.1016/j.atmosenv.2012.07.086>
- Chen Y, Cheng Y, Nordmann S et al (2016a) Evaluation of the size segregation of elemental carbon (EC) emission in Europe: influence



- on the simulation of EC long-range transportation. *Atmos Chem Phys* 16:1823–1835. <https://doi.org/10.5194/acp-16-1823-2016>
- Chen Y, Schleicher N, Fricker M et al (2016b) Long-term variation of black carbon and PM 2.5 in Beijing, China with respect to meteorological conditions and governmental measures \*. *Environ Pollut* 212:269–278. <https://doi.org/10.1016/j.envpol.2016.01.008>
- Chowdhury Z, Zheng M, Schauer JJ et al (2007) Speciation of ambient fine organic carbon particles and source apportionment of PM 2.5 in Indian cities. *J Geophys Res* 112:D15303. <https://doi.org/10.1029/2007JD008386>
- Dubey J, Maharaj Kumari K, Lakhani A (2015) Chemical characteristics and mutagenic activity of PM<sub>2.5</sub> at a site in the Indo-Gangetic plain, India. *Ecotoxicol Environ Saf* 114:75–83. <https://doi.org/10.1016/j.ecoenv.2015.01.006>
- Gupta S, Gadi R, Mandal TK, Sharma SK (2017) Seasonal variations and source profile of n-alkanes in particulate matter (PM 10) at a heavy traffic site. *Delhi Environ Monit Assess* 189. <https://doi.org/10.1007/s10661-016-5756-7>
- Herlekar M, Joseph AE, Kumar R, Gupta I (2012) Chemical speciation and source assignment of particulate (PM10) phase molecular markers in Mumbai. *Aerosol Air Qual Res* 12:1247–1260. <https://doi.org/10.4209/aaqr.2011.07.0091>
- Huma B, Yadav S, Attri AK (2016) Profile of particulate-bound organic compounds in ambient environment of Srinagar: a high-altitude urban location in the North-Western Himalayas. *Environ Sci Pollut Res* 23:7660–7675. <https://doi.org/10.1007/s11356-015-5994-1>
- Jacobson MC, Hansson H-C, Noone KJ, Charlson RJ (2000) Organic atmospheric aerosols: review and state of the science. *Rev Geophys* 38:267–294. <https://doi.org/10.1029/1998RG000045>
- Javed W, Iakovides M, Stephanou EG et al (2019) Concentrations of aliphatic and polycyclic aromatic hydrocarbons in ambient PM 2.5 and PM 10 particulates in Doha, Qatar. *J Air Waste Manag Assoc* 69:162–177. <https://doi.org/10.1080/10962247.2018.1520754>
- Kalaiarasan G, Balakrishnan RM, Sethunath NA, Manoharan S (2018) Source apportionment studies on particulate matter (PM10 and PM2.5) in ambient air of urban Mangalore, India. *J Environ Manag* 217:815–824. <https://doi.org/10.1016/j.jenvman.2018.04.040>
- Kaushal D, Kumar A, Yadav S et al (2018) Wintertime carbonaceous aerosols over Dhauladhar region of North-Western Himalayas. *Environ Sci Pollut Res* 25:8044–8056. <https://doi.org/10.1007/s11356-017-1060-5>
- Kavouras I, Stratigakis N, Stephanou E (1998) Iso- and anteiso-alkanes: specific tracers of environmental tobacco smoke in indoor and outdoor particle-size distributed urban aerosols. *Environ Sci Technol* 32:1369–1377. <https://doi.org/10.1021/es970634e>
- Khan F, Talib M, Hou C et al (2015) Seasonal effect and source apportionment of polycyclic aromatic hydrocarbons in PM<sub>2.5</sub>. 106:178–190. <https://doi.org/10.1016/j.atmosenv.2015.01.077>
- Khedidji S, Balducci C, Ladjji R et al (2017) Chemical composition of particulate organic matter at industrial, university and forest areas located in Bouira province, Algeria. *Atmos Pollut Res* 8:474–482. <https://doi.org/10.1016/j.apr.2016.12.005>
- Kreidenweis SM, Petters M, Lohmann U (2019) 100 years of progress in cloud physics, aerosols, and aerosol chemistry. *Meteorol Monogr*. <https://doi.org/10.1175/amsmonographs-d-18-0024.1>
- Křůmal K, Mikuška P, Večeřa Z (2017) Characterization of organic compounds in winter PM1 aerosols in a small industrial town. *Atmos Pollut Res* 8:930–939. <https://doi.org/10.1016/j.apr.2017.03.003>
- Kumar A, Attri AK (2016) Biomass combustion a dominant source of carbonaceous aerosols in the ambient environment of Western Himalayas. *Aerosol Air Qual Res* 16:519–529. <https://doi.org/10.4209/aaqr.2015.05.0284>
- Latini G, Grifoni RC, Passerini G, Energetic D (2002) Influence of meteorological parameters urban and suburban air pollution. *Air Pollut X*
- Li Z, Porter EN, Sjödin A et al (2009) Characterization of PM2.5-bound polycyclic aromatic hydrocarbons in Atlanta—Seasonal variations at urban, suburban, and rural ambient air monitoring sites. *Atmos Environ* 43:4187–4193. <https://doi.org/10.1016/j.atmosenv.2009.05.031>
- Li Q, Jiang N, Yu X et al (2019) Sources and spatial distribution of PM 2.5-bound polycyclic aromatic hydrocarbons in Zhengzhou in 2016. *Atmos Res* 216:65–75. <https://doi.org/10.1016/j.atmosres.2018.09.011>
- Lyu R, Shi Z, Alam MS et al (2019) Alkanes and aliphatic carbonyl compounds in wintertime PM2.5 in Beijing, China. *Atmos Environ* 202:244–255. <https://doi.org/10.1016/j.atmosenv.2019.01.023>
- Mancilla Y, Mendoza A, Fraser MP, Herckes P (2016) Organic composition and source apportionment of fine aerosol at Monterrey, Mexico, based on organic markers. *Atmos Chem Phys* 16:953–970. <https://doi.org/10.5194/acp-16-953-2016>
- Martins V, Moreno T, Minguillón MC et al (2016) Origin of inorganic and organic components of PM2.5 in subway stations of Barcelona, Spain. *Environ Pollut* 208:125–136. <https://doi.org/10.1016/j.envpol.2015.07.004>
- Masih J, Dyavarchetty S, Nair A et al (2019) Concentration and sources of fine particulate associated polycyclic aromatic hydrocarbons at two locations in the western coast of India. *Environ Technol Innov* 13:179–188. <https://doi.org/10.1016/j.eti.2018.10.012>
- Mikuška P, Křůmal K, Večeřa Z (2015) Characterization of organic compounds in the PM2.5 aerosols in winter in an industrial urban area. *Atmos Environ* 105:97–108. <https://doi.org/10.1016/j.atmosenv.2015.01.028>
- Nirmalkar J, Deshmukh DK, Deb MK et al (2015) Mass loading and episodic variation of molecular markers in PM2.5 aerosols over a rural area in eastern central India. *Atmos Environ* 117:41–50. <https://doi.org/10.1016/j.atmosenv.2015.07.003>
- Novakov T, Andreae MO, Gabriel R et al (2000) Origin of carbonaceous aerosols over the tropical Indian Ocean: Biomass burning or fossil fuels? *Geophys Res Lett* 27:4061–4064
- Pande P, Dey S, Chowdhury S et al (2018) Seasonal transition in PM10 exposure and associated all-cause mortality risks in India. *Environ Sci Technol* 52:8756–8763. <https://doi.org/10.1021/acs.est.8b00318>
- Pankow JF (2001) A consideration of the role of gas/particle partitioning in the deposition of nicotine and other tobacco smoke compounds in the respiratory tract. *Chem Res Toxicol* 14:1465–1481. <https://doi.org/10.1021/tx0100901>
- Pant P, Shukla A, Kohl SD et al (2015) Characterization of ambient PM2.5 at a pollution hotspot in New Delhi, India and inference of sources. *Atmos Environ* 109:178–189. <https://doi.org/10.1016/j.atmosenv.2015.02.074>
- Patel A, Rastogi N (2018) Seasonal variability in chemical composition and oxidative potential of ambient aerosol over a high altitude site in western India. *Sci Total Environ* 644:1268–1276. <https://doi.org/10.1016/j.scitotenv.2018.07.030>
- Petters SS, Petters MD (2016) Surfactant effect on cloud condensation nuclei for two-component internally mixed aerosols. *J Geophys Res Atmos* 121:1878–1895. <https://doi.org/10.1002/2015JD024090>
- Pio CA, Alves CA, Duarte AC (2001) Identification, abundance and origin of atmospheric organic particulate matter in a Portuguese rural area. *Atmos Environ* 35:1365–1375
- Pio CA, Legrand M, Oliveira T et al (2007) Climatology of aerosol composition (organic versus inorganic) at nonurban sites on a west-east transect across Europe. *J Geophys Res* 112. <https://doi.org/10.1029/2006JD008038>
- Pöschl U (2005) Atmospheric aerosols: composition, transformation, climate and health effects. *Angew Chem Int Ed* 44:7520–7540. <https://doi.org/10.1002/anie.200501122>
- Ramachandran S, Rengarajan R, Jayaraman A, et al (2006) Aerosol radiative forcing during clear, hazy, and foggy conditions over a

- continental polluted location in north India. *J Geophys Res Atmos* 111:1–12. <https://doi.org/10.1029/2006JD007142>
- Rinehart LR, Fujita EM, Chow JC et al (2006) Spatial distribution of PM<sub>2.5</sub> associated organic compounds in central California. *Atmos Environ* 40:290–303. <https://doi.org/10.1016/j.atmosenv.2005.09.035>
- Rodríguez S, Querol X, Alastuey A, Plana F (2002) Sources and processes affecting levels and composition of atmospheric aerosol in the western Mediterranean. *J Geophys Res Atmos* 107:1–14. <https://doi.org/10.1029/2001JD001488>
- Rogge WF, Hildemann LM, Mazurek MA, Caw GR (1993) Sources of fine organic aerosol. 2. Noncatalyst and catalyst-equipped automobiles and heavy-duty diesel trucks. *Environ Sci Technol* 27:636–651
- Rogge WF, Hildemann LM, Mazurek MA et al (1994) Sources of fine organic aerosol. 6. Cigarette smoke in the urban atmosphere. *Environ Sci Technol* 28:1375–1388. <https://doi.org/10.1021/es00056a030>
- Roy R, Jan R, Gunjal G et al (2019) Particulate matter bound polycyclic aromatic hydrocarbons: toxicity and health risk assessment of exposed inhabitants. *Atmos Environ* 210:47–57. <https://doi.org/10.1016/j.atmosenv.2019.04.034>
- Sarti E, Pasti L, Scaroni I et al (2017) Determination of n-alkanes, PAHs and nitro-PAHs in PM<sub>2.5</sub> and PM<sub>1</sub> sampled in the surroundings of a municipal waste incinerator. *Atmos Environ* 149:12–23. <https://doi.org/10.1016/j.atmosenv.2016.11.016>
- Schauer C, Niessner R, Pöschl U (2003) Polycyclic aromatic hydrocarbons in urban air particulate matter: decadal and seasonal trends, chemical degradation, and sampling artifacts. *Environ Sci Technol* 37:2861–2868. <https://doi.org/10.1021/es034059s>
- Schnellekreis J, Sklorz M, Peters A et al (2005) Analysis of particle-associated semi-volatile aromatic and aliphatic hydrocarbons in urban particulate matter on a daily basis. *Atmos Environ* 39:7702–7714. <https://doi.org/10.1016/j.atmosenv.2005.04.001>
- Siegrist KJ, Romo D, Upham BL et al (2019) Early mechanistic events induced by low molecular weight polycyclic aromatic hydrocarbons in mouse lung epithelial cells: a role for eicosanoid signaling. *Toxicol Sci* 169:180–193. <https://doi.org/10.1093/toxsci/kfz030>
- Silverstein R, Webster FX, Kiemle D, Bryce D (2014) Silverstein - spectrometric identification of organic compounds 8th ed.pdf. 464
- Tandon A, Yadav S, Attri AK (2008) City-wide sweeping a source for respirable particulate matter in the atmosphere. *Atmos Environ* 42:1064–1069. <https://doi.org/10.1016/j.atmosenv.2007.12.006>
- Tandon A, Rothfuss NE, Petters MD (2019) The effect of hydrophobic glassy organic material on the cloud condensation nuclei activity of particles with different morphologies. *Atmos Chem Phys* 19:3325–3339. <https://doi.org/10.5194/acp-19-3325-2019>
- Thompson CV, Jenkins RA, Higgins CE (1989) A thermal desorption method for the determination of nicotine in indoor environments. *Environ Sci Technol* 23:429–435. <https://doi.org/10.1021/es00181a007>
- Urban RC, Alves CA, Allen AG et al (2016) Organic aerosols in a Brazilian agro-industrial area: speciation and impact of biomass burning. *Atmos Res* 169:271–279. <https://doi.org/10.1016/j.atmosres.2015.10.008>
- Van Drooge BL, Nikolova I, Ballesta PP (2009) Thermal desorption gas chromatography–mass spectrometry as an enhanced method for the quantification of polycyclic aromatic hydrocarbons from ambient air particulate matter. *J Chromatogr A* 1216:4030–4039. <https://doi.org/10.1016/j.chroma.2009.02.043>
- Van Drooge BL, Fontal M, Fernández P et al (2018) Organic molecular tracers in atmospheric PM<sub>1</sub> at urban intensive traffic and background sites in two high-insolation European cities. *Atmos Environ* 188:71–81. <https://doi.org/10.1016/j.atmosenv.2018.06.024>
- Vicente A, Alves C, Monteiro C et al (2011) Measurement of trace gases and organic compounds in the smoke plume from a wildfire in Penedono (central Portugal). *Atmos Environ* 45:5172–5182. <https://doi.org/10.1016/j.atmosenv.2011.06.021>
- Villalobos AM, Amonov MO, Shafer MM et al (2015) Atmospheric pollution. *Atmos Pollut Res* 6:398–405. <https://doi.org/10.5094/APR.2015.044>
- Wan X, Kang S, Xin J et al (2016) Chemical composition of size-segregated aerosols in Lhasa city, Tibetan Plateau. *Atmos Res* 174–175:142–150. <https://doi.org/10.1016/j.atmosres.2016.02.005>
- Wang M, Huang R-J, Cao J et al (2019) Determination of n-alkanes, PAHs and hopanes in atmospheric aerosol: evaluation and comparison of thermal desorption GC-MS and solvent extraction GC-MS approaches. *Atmos Meas Tech Discuss* 12:4779–4789. <https://doi.org/10.5194/amt-12-4779>
- Wilks DS (2006) Statistical methods in the atmospheric sciences. Academic Press, San Diego, pp 463–508
- Yadav S, Tandon A, Attri AK (2013a) Monthly and seasonal variations in aerosol associated n-alkane profiles in relation to meteorological parameters in New Delhi, India. *Aerosol Air Qual Res* 13:287–300. <https://doi.org/10.4209/aaqr.2012.01.0004>
- Yadav S, Tandon A, Attri AK (2013b) Characterization of aerosol associated non-polar organic compounds using TD-GC-MS: a four year study from Delhi, India. *J Hazard Mater* 252–253:29–44. <https://doi.org/10.1016/j.jhazmat.2013.02.024>
- Yadav S, Tandon A, Attri AK (2014) Timeline trend profile and seasonal variations in nicotine present in ambient PM<sub>10</sub> samples: a four year investigation from Delhi region, India. *Atmos Environ* 98:89–97. <https://doi.org/10.1016/j.atmosenv.2014.08.058>
- Yadav S, Tandon A, Tripathi JK et al (2016) Statistical assessment of respirable and coarser size ambient aerosol sources and their timeline trend profile determination: a four year study from Delhi. *Atmos Pollut Res*. <https://doi.org/10.1016/j.apr.2015.08.010>
- Yadav S, Venezia RE, Paerl RW, Petters MD (2019) Characterization of ice-nucleating particles over Northern India. *J Geophys Res-Atmos* 124:10467–10482. <https://doi.org/10.1029/2019JD030702>
- Young L, Wang C (2002) Characterization of n-alkanes in PM<sub>2.5</sub> of the Taipei aerosol. *Atmos Environ* 36:477–482
- Zhang J, Tong L, Huang Z et al (2018a) Seasonal variation and size distributions of water-soluble inorganic ions and carbonaceous aerosols at a coastal site in Ningbo, China. *Sci Total Environ* 639:793–803. <https://doi.org/10.1016/j.scitotenv.2018.05.183>
- Zhang N, Cao J, Li L et al (2018b) Characteristics and source identification of polycyclic aromatic hydrocarbons and n-alkanes in PM<sub>2.5</sub> in Xiamen. *Aerosol Air Qual Res* 18:1673–1683. <https://doi.org/10.4209/aaqr.2017.11.0493>

**Publisher's note** Springer Nature remains neutral with regard to jurisdictional claims in published maps and institutional affiliations.